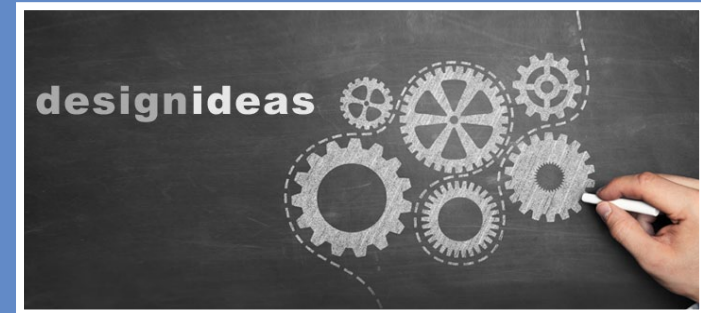
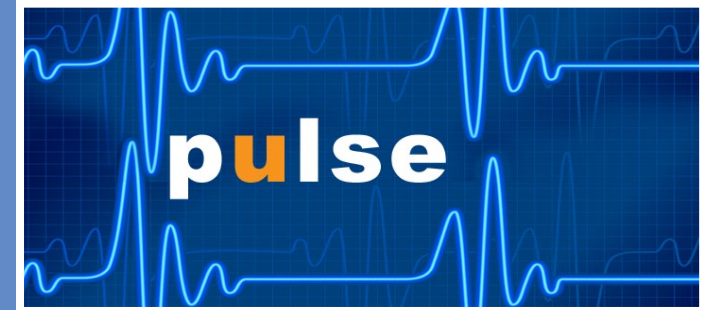


**Imec builds an all-organic microprocessor**



## COVER

### Organic-transistor-based MPU runs at 2 kHz; ROM-coded by ink-jet

**R**esearchers at imec have produced an 8-bit microprocessor that runs at 2.1 kHz. That is not a typing error for GHz; 2.1 kHz is a breakthrough speed in this instance because the transistors that make up the processor's logic are entirely fabricated in low-temperature organic materials. Possible areas of application include high-volume printing of RFID tags.

Belgium's Holst Centre, imec and their partner Evonik have fabricated a general-purpose 8-bit microprocessor using complementary thin-film transistors (TFTs) processed at temperatures up to 250°C, compatible with plastic foil substrates. The microprocessor consists of two separate chips: a processor core chip and a general-purpose instruction generator (P2ROM). For the processor core chip, a complementary hybrid organic-oxide technology was used (p:n ratio 3:1). The general-purpose instruction generator or P2ROM is a one-time programmable ROM memory configured by means of inkjet printing, using a conductive silver ink.

Complete  
article, here



## FEATUREARTICLES

- 12** Design tips for an efficient non-inverting buck-boost converter  
*by Haifeng Fan, Texas Instruments*
- 15** Designing JESD204B converter systems for low BER, Part 2  
*by Jeffrey Ugalde & Ian Beavers, Analog Devices*
- 17** How to measure capacity versus bias voltage on MLCCs  
*by Fons Janssen, Maxim Integrated*
- 20** Precise wireless temperature sensor powers itself  
*By Kris Lokere, Linear Technology*

### ONLINE THIS MONTH;

**GaN: The dawn of a new era?**

*By Janine Love, EDN*

**Embedded security rises and falls with crypto key management**

*by Stephen Evanczuk, EDN*

**Death to "half-power handsets"**

*by Jeremy Hendy, Nujira*

## EDN's columns

- 3 EDN.comment**  
Glimpses of the future leave room for surprises
- 14 Analog Tips**  
A 15-W precision difference amplifier with thermal shutdown  
*by Chau Tran, Analog Devices*
- 19 Teardown**  
A tale of two thermostats: Nest teardown  
*by Richard Quinnell, EDN*
- 31 Review**  
Tektronix RSA306 spectrum analyser  
*by Kenneth Wyatt*
- 26 Product Roundup**  
Power switch with current sensing; low-power FRAM; HMI modules with touch; cute cases for Raspberry Pi
- 21 Design Ideas**
- 22** Three-op-amp state-variable filter perfects the notch
- 24** Series-connected MOSFETs increase voltage & power handling
- 5 Pulse**

# GLIMPSES OF THE FUTURE LEAVE ROOM FOR SURPRISES

As it is the start of a new year, a number of industry bodies have felt moved to share their thoughts on the most significant areas of technological challenge and opportunity that present themselves to us. One such is National Instruments, which has published its [Trend Watch for 2015](#). In a series of short articles, NI looks at several specific topics, from the prospect of 5G communications to the growth of the maker phenomenon. Not unrelated to its instrumentation and test business, NI makes a specific comment on the test environment for coming generations of smart devices, heading this article, “When Exposed to IoT, Big Iron ATE Will Rust.” In that piece, the company argues that, “Traditional automated test equipment (ATE) was optimized to test technology that harnessed the power of Moore’s law – mostly digital, increasing transistor count, decreasing footprint—and it does this very well. But over the past few decades, a subtle shift to integrate more analog technology into ICs has resulted in a test challenge that is much more than Moore. Innovation for the IoT has tasked test engineers to verify mixed-signal systems that include both digital signals and analog signals from sensors, RF antennas, and more – all at consumer volumes and for the lowest price possible. For the testing challenges of tomorrow, traditional ATE falls short. Test engineers need smart ATE for the smart devices of the IoT.”

What NI is leading up to is the contention that just as the consumer products we all use have become adaptable, app-driven and software upgradeable, so too will the test environments that check them out. This reflects, of course, NI’s ongoing product developments in software-defined instrument functions. It may also reinforce – because it’s a mode of thinking that is becoming embedded in the industry – the thought process that bids us ask of all the systems we use; “What if this worked more like a smartphone? Is the traditional operation/use model still the best for this or that product? - and so on. NI also contemplates 5G (whatever form it eventually takes) and how that will inspire thinking, “beyond faster data and greater capacity”; the IIoT, or Industrial IoT – how the connected-device and data analytics era will specifically affect the industrial landscape; and the impact of the maker movement on innovation. You can download NI’s thoughts on the subject from the link above. More futurology, a list of “10 things...” this time, comes from industry analysts IHS, who canvassed opinions on which technologies are most likely to transform the world during the next five years. Here is the list they came up with; 3D printing; Cloud computing/big data; IoT/Internet of Everything; Artificial intelligence; Biometrics; Flexible displays; Sensors; Advanced user interfaces; Graphene; Energy storage and

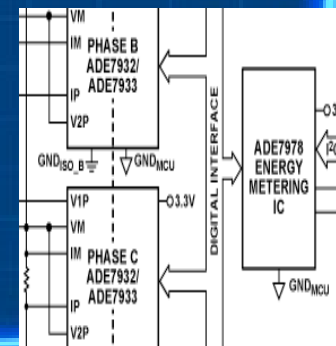
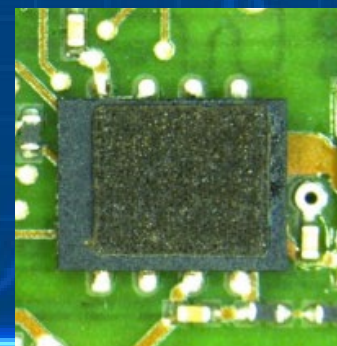
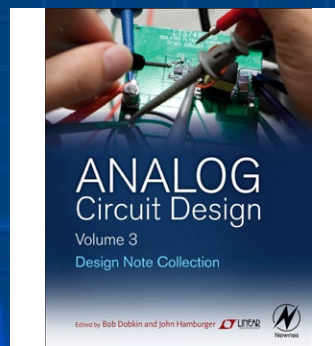
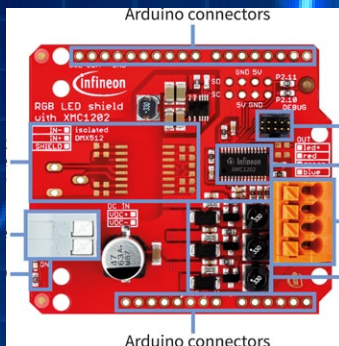
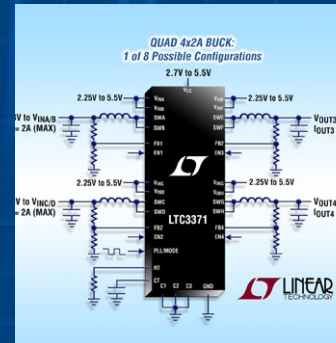
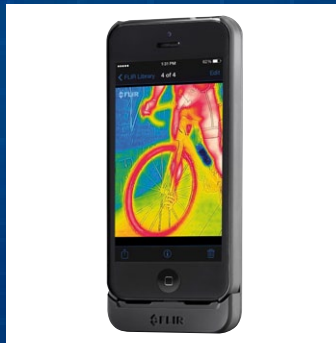
advanced battery technologies.

Does anything surprise you about that list? Perhaps I have been reading too much of this sort of thing, but here’s what surprises me – there are no surprises. It’s exactly the list that probably resides in the desk drawer of every venture capitalist, or, at least, of those that have not abandoned “hard” technology for life sciences and synthetic biology. There are few hints of anything that might spring on us from “left field” and create a major upset. In fact, in some of these areas, technological progress is painfully slow. If, for example, we are ever to have a world powered largely by ambient energy (solar, wind, etc.) we must conquer the energy storage problem. Today’s batteries are far better than they were, but in the context of the energy storage capability we would need to back up really large-scale photovoltaics, they are orders of magnitude away. Other technologies exist... but grid-scale hold-over appears a long way away.

However; no surprises does not mean an absence of good insights and you can [download the paper from IHS](#), following a registration process, to read for yourself. What are the emerging, or rapidly-progressing, areas of technology you expect to most impact you, and your job? In five years, ten years – or even one or two years?



# pulse





## Conductive paint/ink reinvented for the maker generation

**D**istributor RS Components is expanding its offering with products from Bare Conductive; Electric Paint and the company's Arduino-based Touch Board. The products are aimed at the complete range of potential customers, from hobbyists to professional engineers, and including the 'maker' sector.

Electric Paint is a carbon-based paint or ink that comes either in a direct-dispense tube or pen; or in pots for brushing or screening. The product is electrically conductive (in both liquid and dried states), non-toxic, solvent-free, and water-soluble. It can be used as a liquid wire, as a cold-soldering medium, or even as a conductive adhesive, for prototyping, repairing PCBs, and painting circuits and sensors on any surface. It can be used to make ad-hoc connections on any dielectric surface, for example "wiring up" components in education projects by, say, following a circuit drawn on paper.



The medium can be employed as a resistive or capacitive touch sensor; it can be overpainted or placed behind a plastic panel to make it permanent (it air-dries but does not cure and remains water soluble). Quoted resistivity is 55  $\Omega$ /square at 50-microns thickness; clearly, achieved resistance depends on applied thickness and the company says that 32  $\Omega$ /sq is typical for a layer applied by brush. The product screen-prints well, Bare Conductive adds.

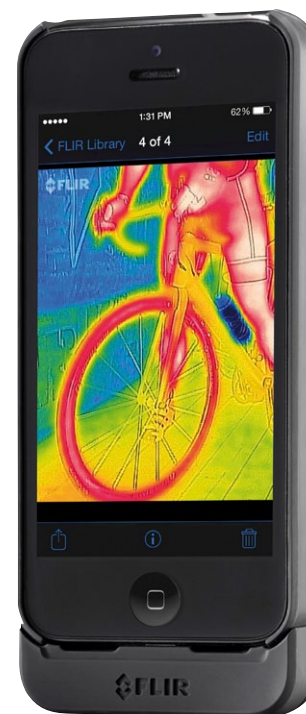
Also from Bare Conductive, RS will be carrying the Touch Board microcontroller board that integrates an Atmel capacitive touch-enabled microcontroller chip, MP3 player, SD Card slot, Li-Po battery charger, and 12 electrodes. The electrodes can be connected directly to conductors, such as Electric Paint pads, to trigger sounds via the MP3 player or other functions such as wireless communication or motor control added using an Arduino expansion shield.

[Complete article, here](#)

## Accessory makes iPhone a thermal imaging camera for the maker generation

**C**onrad Business Supplies has FLIR System Inc's thermal imaging product, the FLIR ONE: it offers the company's expertise in thermography and thermal imaging cameras that enhance perception and awareness - in a pocket-sized format. With

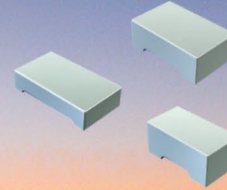
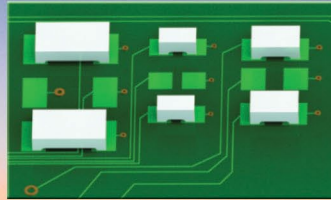
a slim case which attaches to an iPhone 5 or 5s, FLIR ONE turns a smartphone into a thermal infrared camera, giving the ability to "see" and measure minute temperature variations on the phone's screen. Fitted with two cameras, including a long-wave infrared Lepton sensor, the FLIR ONE uses MSX Technology to provide thermal imaging capability and sharpness by blending the thermal and visible spectrum. This technology allows the FLIR ONE to detect temperature differences as small as 0.1  $^{\circ}$ C across a range of 0 $^{\circ}$ C to 100 $^{\circ}$ C. With a dedicated battery, providing four hours of continuous use, the FLIR ONE does not place any additional power demands on the iPhone and it can be charged via a micro USB port.



[Complete article, here](#)

# THiNK™

ZERO OHM SMT JUMPERS



- True Zero ohm jumper • Designed to replace 0603, 0805 and 1206 "Zero" ohm resistor chip sets without changing board designs or layouts
- For high current applications • Low Impedence • Low profile • Manufactured from Copper with Silver plate • Supplied on tape and reel
- Compatible with vacuum pick & place assembly systems • Other chip set sizes available upon request • Request Catalog M60.2

IT'S WHAT'S ON THE INSIDE THAT COUNTS

**KEYSTONE**  
ELECTRONICS CORP.

European Headquarters: [www.keyelco.com](http://www.keyelco.com) • 33 (1) 46 36 82 49 • 33 (1) 46 36 81 57





## Linux systems debugged in the field by embedded execution logging

**R**eversible debugging tools provider Undo Software has introduced Live Recorder, a version of its toolset that assists in debugging Linux systems as they are running, in the field or at an end-customer's site. The product is a two-part offering. The run-time code is instrumented with library elements – Live Recorder – which, when activated, yield log files that can be transferred back to the development team who can apply the UndoDB reversible debugger. Live Recorder allows Linux programs to make a detailed recording of themselves while they are running. The resulting Undo Recording enables developers to debug an exact copy of the original program's execution, allowing them to track down bugs without needing to reproduce them in-house, write test cases or make time-consuming

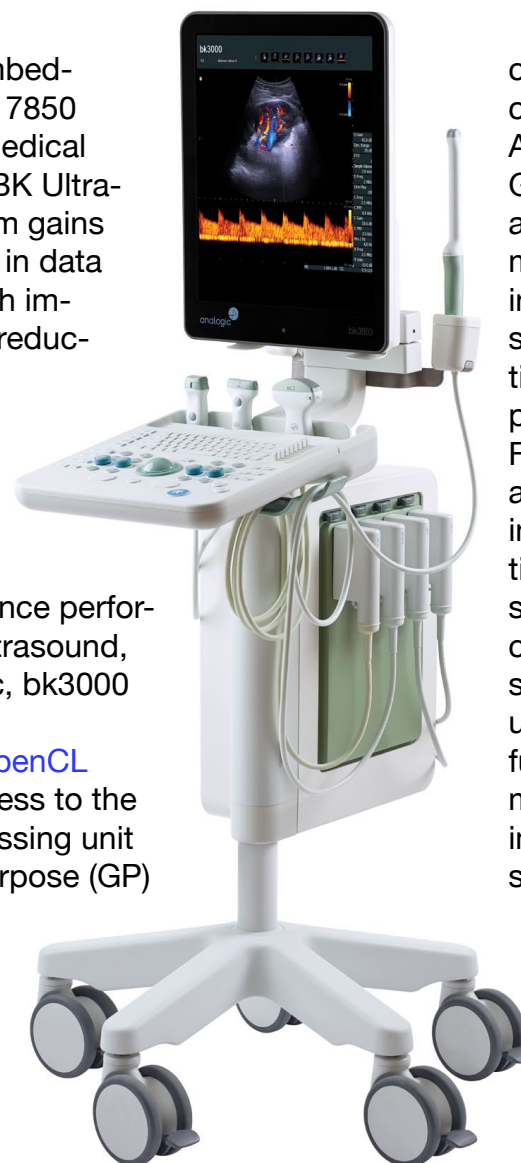
visits to customer sites. Undo Software's debugger allows the code execution to be reproduced and "rewound" – run in exact replica from a chosen point, to reveal the sequences that led to a bug or failure. Software failures in production, the company notes, can be notoriously difficult to fix. The developer does not need to have an exact replica of the end-customer's hardware: code flow will be faithfully recovered on a machine with same generic architecture as the target. By capturing software failures, Live Recorder provides developers with all the information they need to quickly respond to bugs that are found either in the field or internally within their own organisations (such as during software testing).

Complete article, here



## GPGPU & OpenCL boosts medical imaging throughput

**U**sing an AMD Embedded Radeon HD 7850 GPU to accelerate medical imaging, Analogic's BK Ultrasound bk3000 system gains a three-fold increase in data contained within each image, together with a reduction in the time needed to process each scan. In this design-in, AMD's Embedded Radeon HD 7850 GPU is used to enhance performance for the BK Ultrasound, powered by Analogic, bk3000 ultrasound system. Analogic used the [OpenCL standard](#) to gain access to the AMD graphics processing unit (GPU) for general-purpose (GP) computing, referred to as "GP-GPU," delivering performance and offering system and development



cost reduction through cross-platform portability. As a result of using AMD GPU technology, Analogic achieved a 3x improvement in the amount of information in each ultrasound image and reduced time from capture to presentation. Traditional FPGAs and DSPs, AMD asserts, create a fixed, inflexible implementation that requires custom software targeted at specific hardware. Going to a software-based solution using OpenCL helps to further lower the development cost and provides improved long term value since the software can be used across product lines and through generation shifts.

Complete article, here





## Configurable buck DC/DCs: 8A from 2 to 4 independent outputs

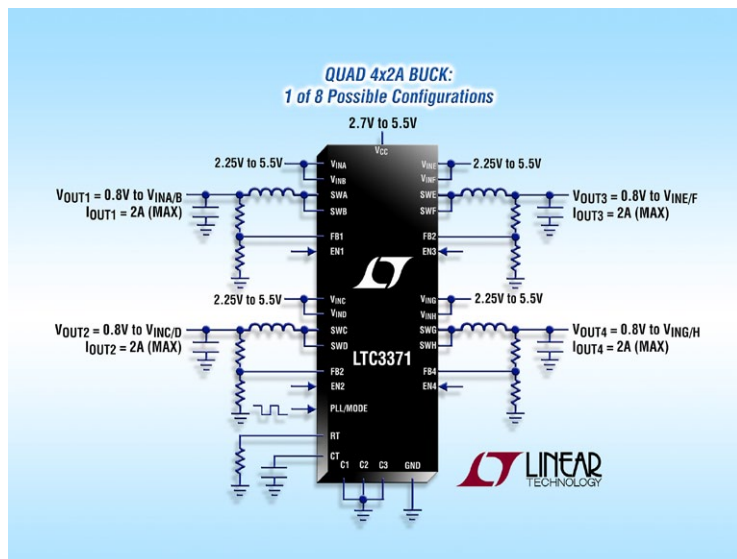
**L**TC3371 is a highly integrated general-purpose power management solution for systems requiring multiple low voltage power supplies. The device features four

across many different applications. The device is suitable for a wide variety of multichannel industrial, automotive, communications and distributed power systems.

The device's buck power stages can be connected in parallel by simply combining their respective VIN and SW pins and programming the desired configuration on the C1-C3 pins. Up to four adjacent power stages can be combined on a single channel, resulting in eight unique output configurations rang-

synchronous buck converters, each powered from independent 2.25V to 5.5V inputs, and each configurable to share up to four of eight available 1A power stages. With eight unique output current configurations, the LTC3371 provides flexibility and ease of reuse

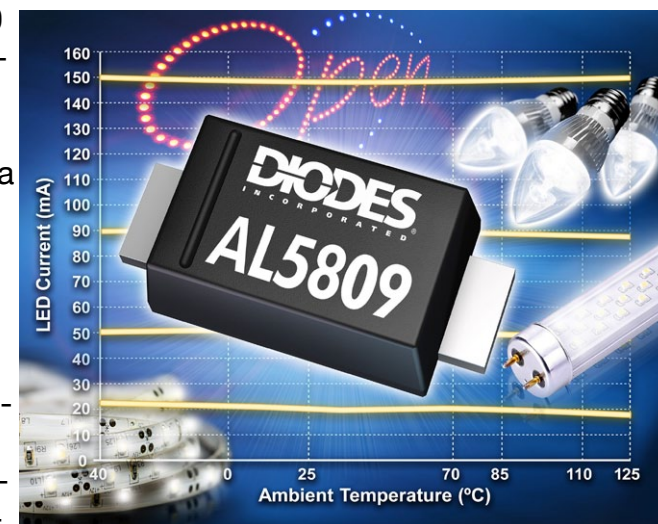
ing from a quad 2A buck to a dual 4A buck. A single inductor may be used for each buck regulator, and any unused power stages may be added to one of the high power channels for improved overall efficiency.



## 2-terminal constant-current linear regulator improves LED current tolerance

**D**iodes Inc's AL5809, a two-terminal PowerDI-123 packaged device, provides an improved accuracy, cost-effective solution for constant-current linear driving of LEDs. With 1.2W maximum power dissipation, 20 ppm/°C temperature stability and high power-supply rejection ratio, the AL5809 delivers LED currents with a  $\pm 5\%$  tolerance over a wide temperature range, greatly simplifying the solutions for its target applications of LED signage, LED strip lighting and low-current retrofit lamps. The AL5809 is a small footprint, low BOM-cost LED driver that is simple

to use and provides improved accuracy and all-round higher performance than competitive alternatives or discrete circuit designs. The AL5809 is specified for the  $-40^{\circ}\text{C}$  to  $+125^{\circ}\text{C}$  temperature range, with an operating voltage (between the two terminals) from



to use and provides improved accuracy and all-round higher performance than competitive alternatives or discrete circuit designs. The AL5809 is specified for the  $-40^{\circ}\text{C}$  to  $+125^{\circ}\text{C}$  temperature range, with an operating voltage (between the two terminals) from

2.5V to 60V and is offered in various fixed-output current versions from 15 to 150 mA; this removes the need for external current setting resistors. As well as meeting the needs of designs requiring a simple linear regulator (e.g., no inductor or external resistor), the AL5809 provides additional performance features; over-temperature protection (OTP) and the ability to drive both low- and high-side LED chains.

Complete article, here

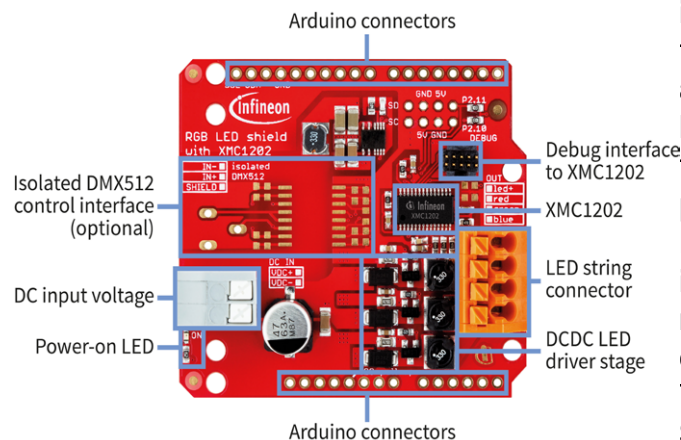


Complete article, here



## Arduino shields for RGB lighting and motor control from Infineon

Infineon Technologies has added two shields for Arduino designs; both are compatible to Arduino



Uno R3 and can be combined with the XMC1100 Boot Kit which is equipped with a 32-bit microcontroller from the XMC1000 family. All XMC1000 products use the ARM Cortex-M0 processor. The Infineon RGB LED Lighting Shield for Arduino hosts the XMC1202 microcontroller with its Brightness Colour Control Unit (BCCU) for LED lighting control. The high-current DC Motor Control Shield for Arduino contains the Infineon NovalithIC

BTN8982TA, an integrated half-bridge driver for motor control. The RGB LED Lighting Shield is an intelligent evaluation board for Arduino. It allows the adoption of different LED light engines to ensure fast prototyping and inexpensive evaluation. The Lighting Shield has three independent output channels for flicker-free control of multicolour LEDs.

The DC Motor Control Shield with BTN8982TA for Arduino enables fast and cost-effective prototyping of DC motor control designs with easy testing of half-bridge and full-bridge motor control applications. The Motor Control Shield is capable of driving two uni-directional DC motors or one bi-directional DC motor. The Shield implements two NovalithIC BTN8982TA fully integrated high-current half-bridge drivers for motor drives.

Complete article, here



## 15 Watt Qi-compliant wireless charging

Enabling faster charging than conventional USB and other wired technologies, and supporting rapid recharging for tablets, hand-held medical devices and other larger devices, Freescale Semiconductor has extended its wireless charging with what it claims as the first 15-W Qi-compliant wireless charging solution. This chipset comprises two 15W ICs: the WPR1516 receiver chip and accompanying MWCT1012 transmitter chip, which come with firmware libraries. The solution also includes an application programming interface that can be used to modify or adjust library functionality, allowing for the addition of custom application code and a highly tailored and differentiated end-product.

There is a production-ready reference design, and evaluation boards. To support the WPR1516 receiver IC, Freescale provides two evaluation board options for different output power topologies, WPR1500-LDO and WPR1500-



BUCK. The MWCT1012 transmit controller IC is supported with the WCT-15W1COILTX reference design.

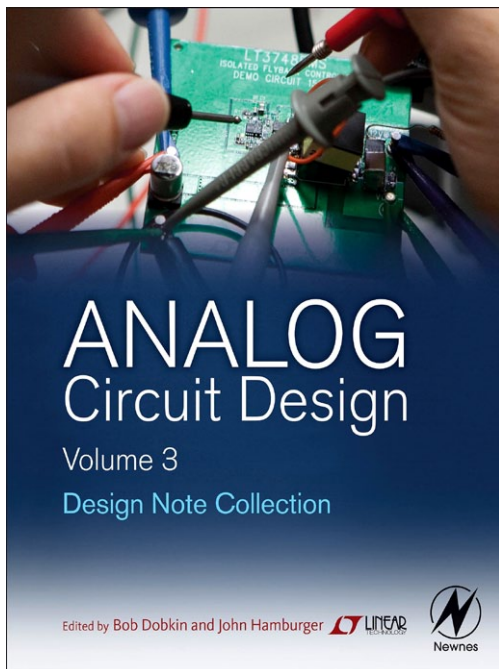
Complete article, here





## “Analog Circuit Design, Volume Three”

Published by Elsevier, “Analog Circuit Design Volume Three: Design Note Collection” – edited by ana-

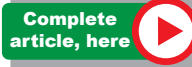


logue circuit design leader, Linear Technology’s Bob Dobkin – is the next book in the Analog Circuit Design series.

The [Design Note Collection](#) is a comprehensive volume of applied circuit design solutions, providing

refined and practical design techniques. The book includes an extensive power management section, covering switching regulator design, linear regulator design, microprocessor power design, battery management, powering LED lighting, automotive and industrial power design. Other sections span a range of analogue design topics, including data conversion, data acquisition, communications interface design, operational amplifier design techniques, filter design, wireless/RF communications and network design.

This book is 1136 pages in length and is available as an e-book, or a hardcover print version (in January 2015). This book extends the series initiated by the successful publication of [“Analog Circuit Design: A Tutorial Guide to Applications and Solutions”](#) and [“Analog Circuit Design, Volume 2, Immersion in the Black Art of Analog Design”](#).

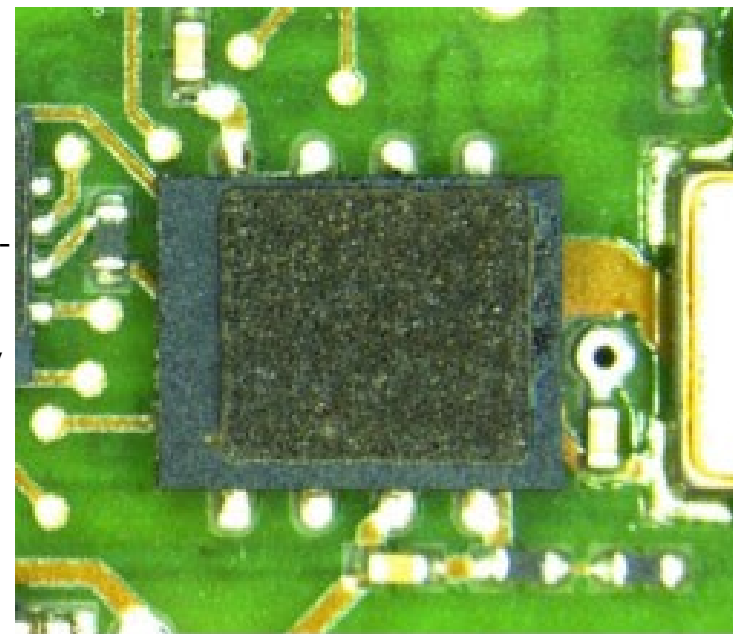


## Obscured part numbers protect IP without the grind of grinding

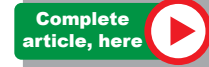
Companies frequently require markings on components to be removed to make it hard for rivals to easily find out what parts are used on the PCB. Contract manufacturer Escatec has developed a technique using an existing production machine, that simplifies the task and eliminates stress to components. The usual technique of manually grinding the markings off is time consuming and is liable to damage components and stress solder joints. Escatec has solved this problem by using

its existing CO2 laser marker that was initially installed to change the surface structure of solder resist to give a clear and permanent marking on the surface of PCBs. “We found that using the laser to burn on a ‘sea of numbers’ pat-

tern on the tops of the components made sure that none of the [manufacturers’ original] markings can be read,” explained Martin



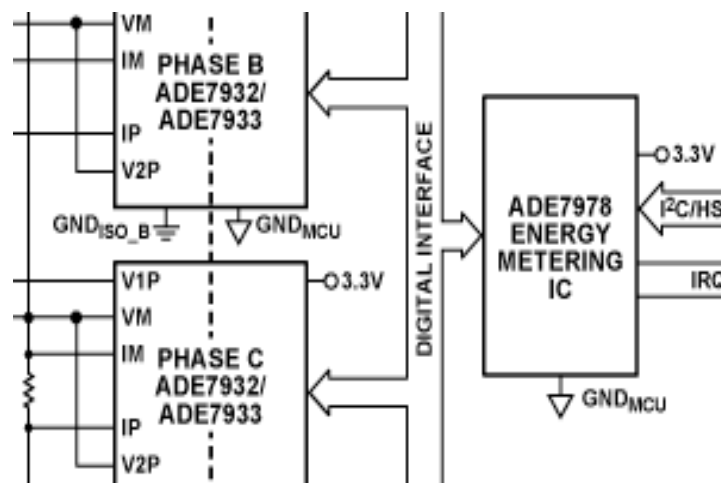
Muendlein, Engineering Manager at Escatec. “There is no damage or stress and the laser is very fast and accurate to within  $\pm 0.1$  mm.”





## Chipset measures complete set of 3-phase AC power parameters

Analog Devices has posted details of a chipset specifically designed for measuring 3-phase electrical



energy, using shunts as current sensors. The chipset comprises the ADE7978, the ADE7933/ADE7932, and ADE7923. ADE7933/ADE7932 are isolated, 3-channel sigma-delta analogue-to-digital converters ( $\Sigma\Delta$  ADCs) for polyphase energy metering applications that use shunt current sensors. The ADE7923 is a non-isolated, 3-channel  $\Sigma\Delta$  ADC for the neutral line that uses a shunt

current sensor. The ADE7932 features two 24-bit ADCs, and the ADE7933 and ADE7923 feature three 24-bit ADCs. One channel is dedicated to measuring the voltage across the shunt when a shunt is used for current sensing. This channel provides a signal-to-noise ratio (SNR) of 67 dB over a 3.3 kHz signal bandwidth. Up to two additional channels are dedicated to mea-

suring voltages, which are usually sensed using resistor dividers. The unused voltage channels on the neutral ADE7923 can be used for auxiliary voltage measurements. These channels provide an SNR of 75 dB over a 3.3 kHz signal bandwidth. One voltage channel can be used to measure the temperature of the die via an internal sensor.

[Complete article, here](#)

## SSL/TLS secure-socket code for embedded devices

Segger's emSSL is a ground-up implementation of secure sockets that are the backbone of secure communications on the Internet today. Written to run on single-chip embedded devices, emSSL integrates seamlessly with embOS/IP or, alternatively, any IP stack that supports plain sockets, or any bidirectional communications channel. emSSL supports TLS version 1, 1.1, and 1.2 out of the box and provides modern cipher suites that offer robust authentication, confidentiality, message integrity, and forward secrecy. Whilst being compact, it is also efficient in terms of RAM, ROM, and processor load. emSSL's highly flexible and straightforward configuration targets small devices by linking only what's necessary, and at the same time avoids a sea of preprocessor defines that drown other source code products. "emSSL cements our intention to



strengthen and augment Segger middleware with modern security features demanded by our industrial customers," says Rolf Segger, owner and CTO of Segger.

[Complete article, here](#)

## DESIGN TIPS FOR AN EFFICIENT NON-INVERTING BUCK-BOOST CONVERTER

By Haifeng Fan, Texas Instruments

This article presents operational principles, current stress and power-loss analysis of several common buck-boost converters, and presents design criteria for an efficient non-inverting buck-boost converter.

Buck-boost (step-down and step-up) converters are widely used in industrial personal computers (IPCs), point-of-sale (POS) systems, and automotive start-stop systems. In these applications, the input voltage could be either higher or lower than the desired output voltage. A basic inverting buck-boost converter has a negative output voltage with respect to ground. The single-end primary inductor converter (SEPIC), Zeta converter, and two-switch buck-boost converters have positive or non-inverting outputs. However, compared with a basic inverting buck-boost converter, all three non-inverting topologies have additional power components and reduced efficiency. This article presents operational principles, current stress and power-loss analysis of these buck-boost converters, and presents design criteria for an efficient non-inverting buck-boost converter.

### Inverting buck-boost converter

Figure 1 shows the schematic of a basic in-

verting buck-boost converter, along with the typical voltage and current waveforms in continuous conduction mode (CCM). In addition to input and output capacitors, the power stage consists of a power MOSFET, a diode, and an inductor. When the MOSFET (Q1) is ON, the voltage across the inductor ( $L_1$ ) is  $V_{IN}$ , and the inductor current ramps up at a rate that is proportional to  $V_{IN}$ . This results in accumulating energy in the inductor. While Q1 is ON, the output capacitor supplies the entire load current. When the Q1 is OFF, the diode (D1) is forward-biased and the inductor current ramps down at a rate proportional to  $V_{OUT}$ . While Q1 is OFF, energy is transferred from the inductor to the output load and capacitor.

The voltage conversion ratio of an inverting buck-boost in CCM can be expressed as:

$$M = \frac{V_{OUT}}{V_{IN}} = -\frac{D}{1-D}, \quad (1)$$

where  $D$  is the duty cycle of Q1 and is always in a range of 0 to 1. Equation 1 indicates that the magnitude of output voltage could be either higher (when  $D > 0.5$ ) or lower (when  $D < 0.5$ )

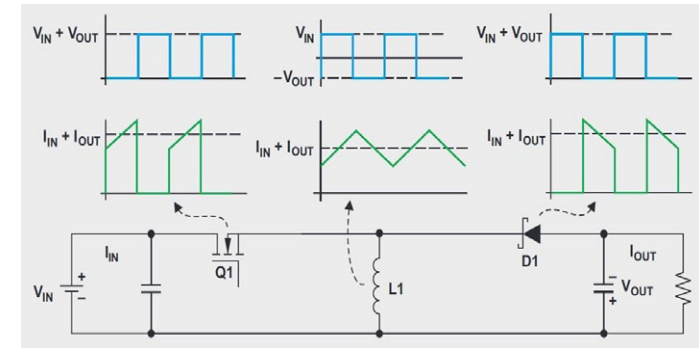


Figure 1. Inverting buck-boost converter

than the input voltage. However, the output voltage always has an inverse polarity relative to the input.

### Conventional non-inverting buck-boost converters

The inverting buck-boost converter does not serve the needs of applications where a positive output voltage is required. The SEPIC, Zeta, and two-switch buck-boost converter are three popular non-inverting buck-boost topologies. The Zeta converter, also called inverse SEPIC, is similar to SEPIC, but less attractive than SEPIC since it requires a high-side driver that increases the circuit complexity.

A SEPIC converter and its ideal waveforms in CCM are shown in Figure 2. The voltage conversion ratio of a SEPIC converter is:

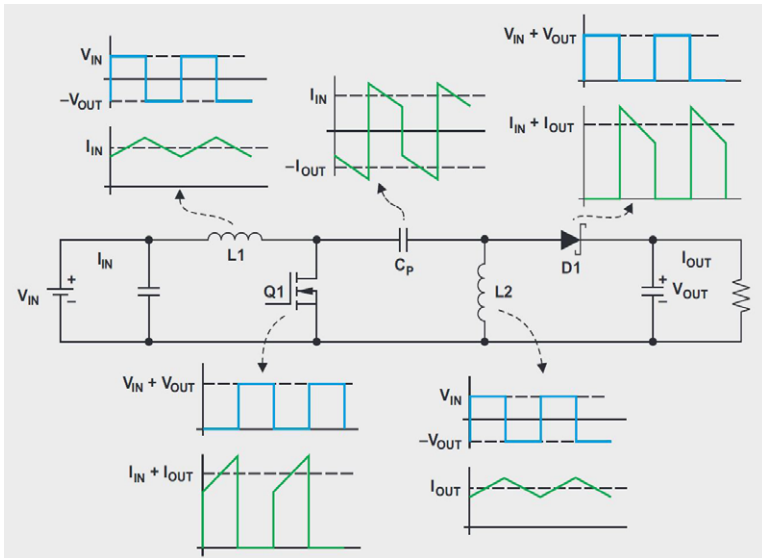


**Figure 2.** SEPIC converter

$$M = \frac{V_{OUT}}{V_{IN}} = \frac{D}{1-D} \quad (2)$$

Equation 2 indicates a positive output voltage and the buck-boost capability.

Like an inverting buck-boost converter, a SEPIC converter has a single MOSFET (Q1) and a single diode (D1). The MOSFET and diode in a SEPIC converter have voltage and current requirements similar to their counterparts in an inverting buck-boost

converter. As such, the power losses of the MOSFET and diode are similar. On the other hand, a SEPIC converter has an additional inductor (L2) and an additional AC-coupling capacitor (Cp).

In a SEPIC converter, the average inductor current of L1 equals the input current ( $I_{IN}$ ), whereas the average inductor current of L2 equals the output current ( $I_{OUT}$ ). In contrast, the single inductor in an inverting buck-boost converter has an average current of  $I_{IN} + I_{OUT}$ . The coupling capacitor sees significant root-mean-square (RMS) current relative to both input current and output current, which generates extra power loss and reduces the converter's overall efficiency.

To reduce power loss, ceramic capacitors with low equivalent series resistance (ESR) are desired, which usually leads to higher cost. The additional inductor of a SEPIC converter, coupled with the extra coupling capacitor, increases PCB size and total solution cost. A coupled inductor can be used to replace two separate inductors to reduce PCB size. However, the selection of off-the-shelf coupled inductors is limited when compared to separate inductors. Sometimes a custom design will be required, which increases cost and lead time.

*The continuation of this article discusses the two-switch buck-boost converter and its optimisation – click below for the full article pdf download.*



**Download PDF  
of Article**



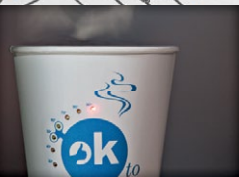
**Find non-inverting buck-boost  
on EETsearch**

**The No.1 Event for Printed Electronics**

**Exhibition: March 4–5, 2015**  
**Conference: March 3–5, 2015**  
**Messe München, Germany**



**LOPEC**  
Printed Electronics –  
We Build the Market



**LOPEC**

[www.lopec.com](http://www.lopec.com)

**7th International Exhibition  
and Conference for the  
Printed Electronics Industry**



# A 15-W PRECISION DIFFERENCE AMPLIFIER WITH THERMAL SHUTDOWN

BY CHAU TRAN, ANALOG DEVICES

This precision amplifier can source or sink 1A, making it ideal for high-power applications such as component stereos, self-powered speakers, and home theatres.

Many applications require both high precision and high output current. A simple way to provide both is to combine a precision amplifier with a power amplifier. Placing an ADA4870 high-power amplifier inside the feedback loop of an AD8271 precision difference amplifier allows the circuit to provide the high output current of the ADA4870 while maintaining the DC precision of the AD8271. The output buffer can easily source 1A; the high-precision, low-distortion preamp with trimmed on-chip resistors provides lower gain drift and gain error, and higher common-mode rejection, than discrete designs.

The ADA4870 draws about 30 mA, but a power saving shutdown fea-

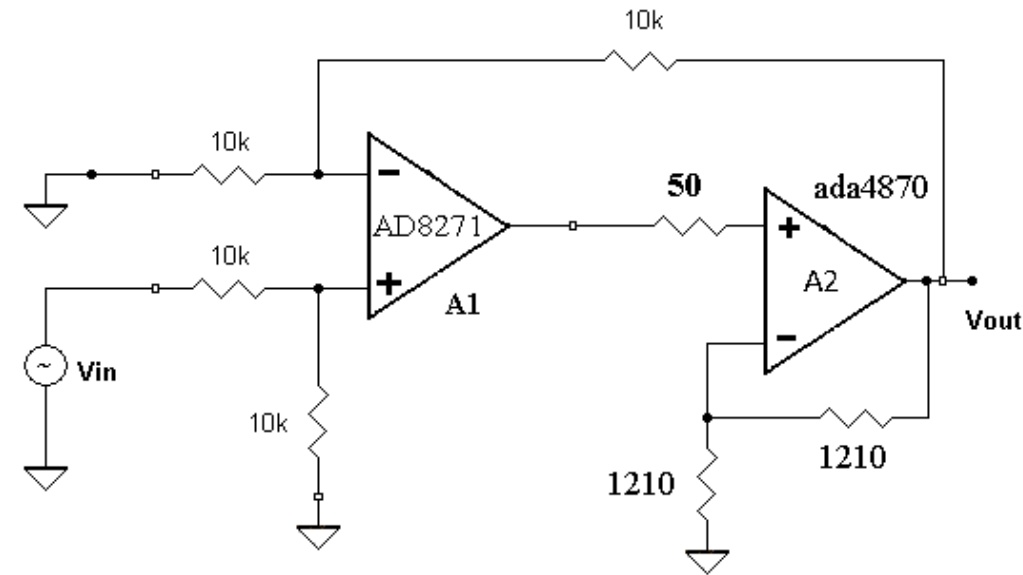



Figure 1. High-power difference amplifier.

ture reduces the quiescent current to approximately 750  $\mu$ A. Simply pull the shutdown pin low and the circuit turns off. High output current amplifiers generate heat, causing the die temperature to increase, so a heat sink will be typically be required to improve the long-term reliability and keep the die temperature at a

level such that the thermal protection circuitry is not activated under normal circumstances.

In addition to short-circuit protection, the ADA4870 is protected against excessive die temperatures. When detected, the amplifier switches to an off state, dropping the supply current to approximately 5 mA. When the die temperature returns to an acceptable level, the amplifier automatically resumes normal operation. This thermal protection mode is very useful to prevent long-term thermal stress of the circuit. A device can heat up to a relatively high temperature if the fault condition is temporary. This greatly reduces the stress imposed by thermal cycling, which in turn improves its reliability under sustained fault conditions.

**Chau Tran** [chau.tran@analog.com] joined Analog Devices in 1984 and works in the Integrated Amplifier Products (IAP) Group in Wilmington, MA. In 1990, he graduated with an MSEE degree from Tufts University. Chau holds more than 10 patents and has written more than 10 technical articles.



## DESIGNING JESD204B CONVERTER SYSTEMS FOR LOW BER, PART 2

By Ian Beavers & Jeffrey Ugalde, Analog Devices

With the adoption of the new high speed serial digital interface link, known as JESD204B, between converters and FPGAs, the error rate within the digital transmission line cannot be ignored as a potential contributor to the overall BER. Part 2 of this article continues the discussion;

### JESD204B lane traces: how long is too long?

Figure 6 shows other eye diagrams with the JESD204B receiver eye mask. The plots depict the effects of conductor loss of the same 12.5 Gbps PRBS7 signal in 370HR PCB material for different channel lengths. There is a direct correlation between insertion loss caused by different channel lengths and the amount of data eye closure relative to the mask for the same PCB material. In this example, the shortest channel length of 1 in. (2.5 cm) has the least measured insertion loss. This produces the best eye opening while the longest channel length of 12 in. (30 cm) produces the worst eye opening.

In the two examples above, the combined effects of timing jitter and amplitude noise as a function of insertion loss can be seen. As insertion loss increases, so does the relative timing jitter and amplitude noise. This reduces the

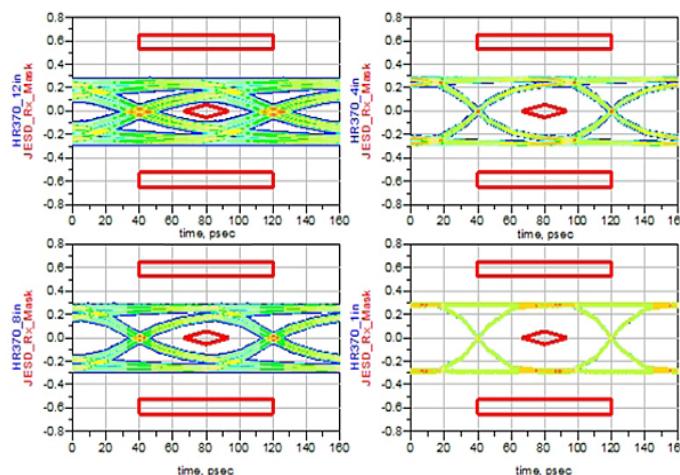


Figure 6. 12.5 Gbps Eye diagrams of 370HR material using varying channel lengths.

eye opening available for data sampling. Ideally, the best location to sample the data is at the middle of the data mask. However, JESD204B receivers need some margin in the time axis and the voltage axis to correctly capture each bit. Therefore, as the eye opening is closed, the probability of capturing and resolving an incorrect bit goes up. This will affect the bit error rate of the link.

The effect of data rate to timing jitter and amplitude noise for a constant channel length is also important for maintaining a low bit er-

ror rate. As data rate decreases, the data eye opening will increase since the high frequency components at a slower data rate exhibit less insertion loss from the channel. Higher data rates will correspondingly decrease the available data eye opening.

Figure 7 compares the eye opening seen at the receiver, scaled to its corresponding UI (unit interval). The eye for a 6.25 Gbps data rate has less relative timing jitter and amplitude noise than the 12.5 Gbps data rate. These examples show how the conductor loss and dielectric loss affects the eye opening and therefore affects the potential bit error rate of the JESD204B link.

Material quality and design techniques such as loosely coupled differential traces help improve insertion loss. This helps improve the eye opening and therefore improves the bit error rate of the link.

### Best layout practices to minimise BER

Depending on the application and its sensitivity to cost and area, there are layout practices to consider for JESD204B high speed serial transmission lines in order to minimise channel loss and mitigate the bit error rate.

- High speed SERDES channel traces over 12 inches (30 cm) in length operating at high bit rates of 12.5 Gbps are typically best routed on higher grade PCB material, as cost permits.

# SERIAL INTERFACING

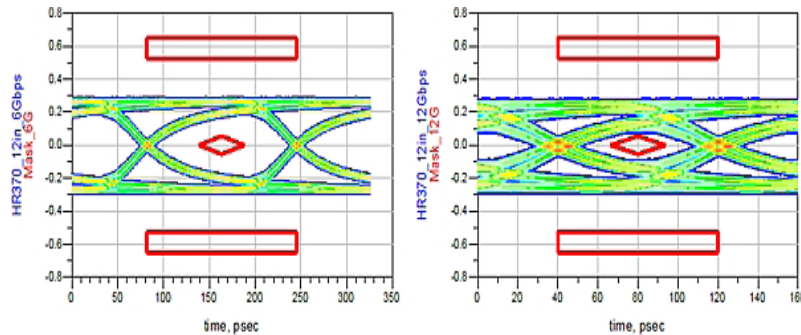


**Figure 7.** 6.25 Gbps (left) and 12.5 Gbps (right) eye diagrams using 370HR material with the JESD204B receiver Mask

Better quality PCB material will reap the benefit of lower channel loss.

- Channel traces under 12 inches of length operating at high bit rate should be acceptable in lower-grade PCB material, where emphasis and equalisation can be used to improve bit error rate of the JESD link.

- It is commonly believed that 100Ω differential signals require differential traces. Differential signals can be perfectly well routed on two 50Ω single-ended traces. This is known as a “loosely coupled” differential pair. Loosely coupled differential pairs are typically a differential pair where

the edge-to-edge spacing between signal pairs is at least three times that of the trace width.

- Tightly coupled differential pairs are differential pairs where the edge-to-edge spacing is less than 3x that of the trace width.
- Wider spacing on differential pairs has a lower conductor loss due to increased surface area for skin effect. In the case where signal loss is important, which is typically on long traces, high data

rates, and with lower grade PCB material, loosely coupled differential traces are essential.

- Interconnects, vias and sharp 90-degree corners in transmission lines typically affect the characteristic impedance of the channel, and any deviation from the designed characteristic impedance will result in unwanted reflections in the transmitted signal. Avoid using vias as much as possible in high speed differential traces.

*Read the complete article, plus Part 1, in the pdf download, click below.*



**Download PDF  
of Article**

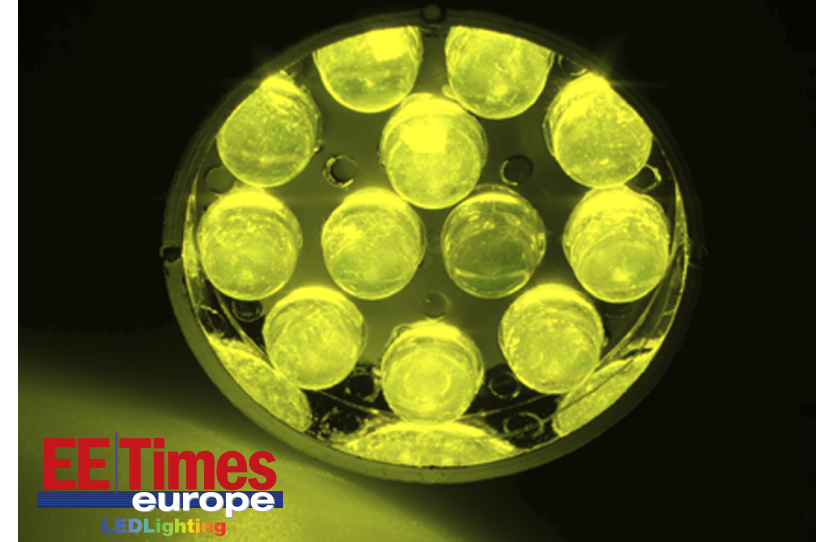


**Find JESD204B converter  
systems on EETsearch**

## Automotive Electronics



## LEDLighting





## HOW TO MEASURE CAPACITY VERSUS BIAS VOLTAGE ON MLCCS

By Fons Janssen, Maxim Integrated

High-capacity, multilayer ceramic capacitors (MLCC) have a property often not well understood by electronic designers: the capacitance of these devices varies with applied DC voltage. This phenomenon is present in all high-dielectric constant, or Class II capacitors (B/X5R R/X7R, and F/Y5V characteristic).

The amount of variation can differ considerably among different MLCC types. A good article on this topic was written by Mark Fortunato.[Ref. 1] The conclusion of that article is that you should always check the capacitor's datasheet to see how the capacitance varies with the bias voltage. But what if the datasheet does not include this information? How can you determine how much capacitance is lost under the conditions in your application?

### Theory for characterising capacitance vs. bias voltage

A circuit to measure the DC bias characteristic is shown in Figure 1.

This circuit is built around op amp U1 (MAX4130). The op amp acts as a comparator, with feedback resistors R2 and R3 adding hys-

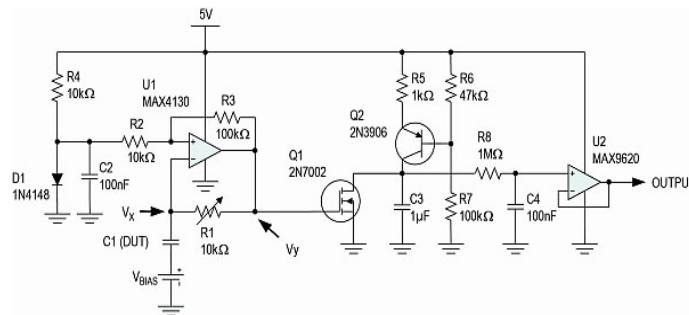


Figure 1. Circuit to characterise capacitance versus bias voltage.

teresis. D1 sets a threshold above GND so that no negative supply voltage is needed. C1 and R1 form a feedback network to the negative input, which makes the circuit operate as an RC oscillator. Capacitor C1, the device under test (DUT), serves as the C in this RC oscillator; potentiometer R1 is the R.

The voltage waveforms of the op amp output pin, Vy, and the junction between R and C, Vx, are shown in Figure 2. When the output of the op amp is at 5V, capacitor C1 is charged by R1 until it reaches the upper threshold. This forces the output to 0V. Now the capacitor is discharged until Vx reaches the lower threshold, thus forcing the output back to 5V. This process repeats, resulting in a stable oscillation.

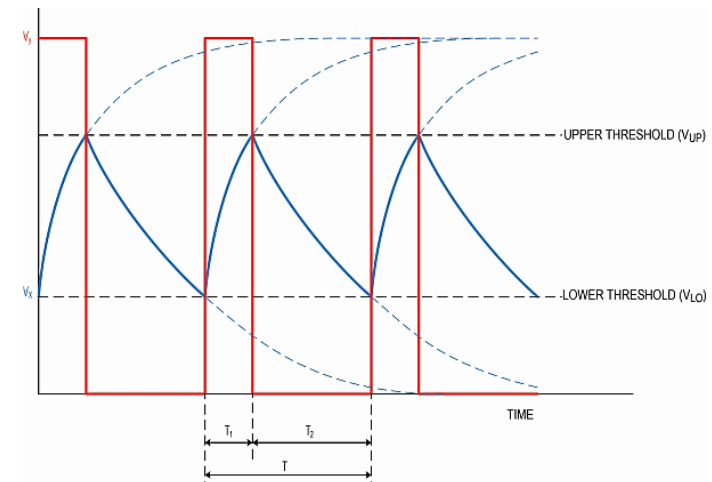


Figure 2. Oscillation voltages  $V_x$  and  $V_y$

The oscillation period depends on the values of R, C, and the upper and lower thresholds  $V_{UP}$  and  $V_{LO}$ :

$$T_1 = RC \ln \left( \frac{5V - V_{LO}}{5V - V_{UP}} \right) = \alpha RC$$

$$T_2 = RC \ln \left( \frac{V_{UP}}{V_{LO}} \right) = \beta RC$$

$$T_1 = \frac{\alpha}{\beta} T_2$$

$$T = T_1 + T_2 = \left( 1 + \frac{\alpha}{\beta} \right) T_2$$

# SERIAL INTERFACING

Since 5V,  $V_{UP}$  and  $V_{LO}$  are constant, then  $T_1$  and  $T_2$  are proportional to RC. (This is often referred to as the RC time constant.)

The threshold of the comparator is a function of  $V_y$ , R2, R3, and the forward voltage of D1 ( $V_{DIODE}$ ):

$$V_{THRESHOLD} = V_{Diodes} \frac{R3}{R2 + R3} + V_y \frac{R2}{R2 + R3}$$

Where  $V_{UP}$  is the threshold for  $V_y = 5V$ , and  $V_{LO}$  is the threshold for  $V_y = 0V$ . With the given values these thresholds yield to approximately 0.55V for  $V_{LO}$ , and 1.00V for  $V_{UP}$ .

The circuit around Q1 and Q2 converts the cycle time into a proportion-al voltage, which is used to indicate the effective capacitance with differ-ent applied voltages.

*The continuation of this article enlarges on how the circuit works, and produces results confirming the validity of the approach – click below for pdf download.*



**Download PDF  
of Article**



**Find MLCCs on EETsearch**

## smartsystems integration



International Conference and Exhibition  
on Integration Issues of Miniaturized Systems  
– MEMS, NEMS, ICs and Electronic Components

**Copenhagen, Denmark, 11–12 March 2015**  
[smartsystemsintegration.com](http://smartsystemsintegration.com)

### BE PART OF IT!

*Knowledge exchange  
Trends and innovations  
Networking*

#### Main conference topics:

- Smart energy systems
- Smart Medtech systems
- Smart production
- System integration and packaging

**Register now at**  
[smartsystemsintegration.com/registration](http://smartsystemsintegration.com/registration)

Co-organizer:



Part of the activities of:



**Contact:**  
**+49 711 61946-292**  
**[smart@mesago.com](mailto:smart@mesago.com)**

**mesago**  
Messe Frankfurt Group

## A tale of two thermostats: Nest teardown

**H**ome automation is the application where many consumers are getting their first introduction to the Internet of Things (IoT), so it seemed appropriate to explore how vendors are approaching device design in this market. I selected two devices to explore. One was the Nest thermostat, which generated considerable buzz in the market when it came out a few years ago. The other was a more recent introduction: the Honeywell smart WiFi thermostat.

To see how the two compare when digging further inside, I began at the outer layer.

The Honeywell provides a full-colour touchscreen for controlling its operation. One attribute of this feature is that you can select the background colour to complement the colour scheme of your house. The Nest thermostat has a look resembling that of conventional



electromechanical thermostats, with a simple colour display that indicates current and set point temperature, colour coded to show if it is heating or cooling. It senses the user's presence, lighting up when approached but darkening when not needed.

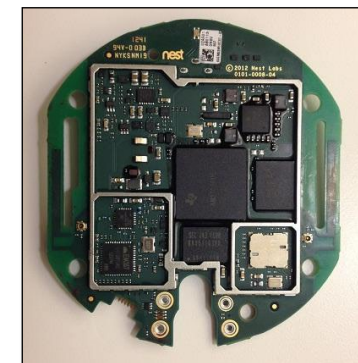
Unlike the touchscreen of the Honeywell, the Nest has users rotate the outer ring to identify the action they wish to take, then press the unit to confirm the selection. Audible clicks accompany these actions to provide haptic feedback.

The Honeywell wall plate is a simple two-layer PCB with connectors for the wires coming from the HVAC unit. The Nest wall plate has active components, including an STMicro STM32L151 microcontroller and an 8-channel analog Mux. The bubble level in the centre is there to aid in proper installation of the back plate to the wall.

The Honeywell unit's single PCB includes DC-DC converters, voltage regulators, rectifiers, an 8-channel, 12-bit ADC, 128 MB of SDRAM, 32M

of Flash, and a Broadcom WiFi module (shield removed). An Atmel 926 ARM processor is the main processing unit, enclosed by the metal shield just visible underneath the flat-ribbon cable to the display.

The main board of the Nest, with metal shield removed, shows a TI Sitara CPU, power management and USB chip, Flash, 32Mx16 SDRAM, and a Murata WiFi module. There is also a ZigBee network coprocessor, implying that the device may offer expansion options in the future.



Complete article, here 



# WIRELESS SENSORS

## PRECISE WIRELESS TEMPERATURE SENSOR POWERS ITSELF

By Kris Lokere, Linear Technology Corp.

The “Internet of Things” refers to a growing trend to connect not only people and computers, but all sorts of “things” to the Internet. In applications such as industrial plants or large infrastructure projects, connecting more sensors (or actuators) in more places can increase efficiency, improve safety, and enable entirely new business models.

Rather than the challenge and expense of running cables all around a factory, it is now possible to install reliable, industrial-strength wireless sensors that can operate for years on a small battery, or even harvest energy from sources that are already available, such as light, vibration, or temperature gradients.

This case study shows a real-world design that combines a high-resolution temperature sensor, a power management circuit that uses solar energy when available and battery backup when needed, and a low-power radio module that automatically forms a reliable mesh network to wirelessly connect all sensors to a central access point.

Design overview

Figure 1 shows the block diagram of the design. The temperature sensor is based on a

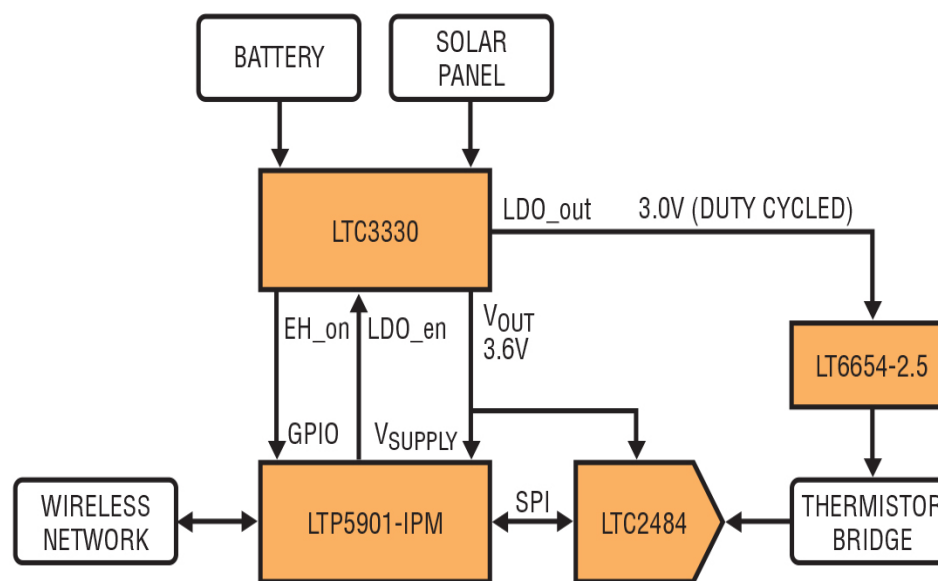


**Figure 1.** A wireless temperature sensor is formed by connecting a wireless radio module to an ADC, reference and thermistor. The circuit is powered by an energy harvester that can take power from a battery or solar panel.

thermistor biased by a low noise LT6654 voltage reference. The 24-bit delta-sigma ADC

LTC2484 reads the thermistor voltage and reports the result via SPI interface. The LTP5901 is the radio module that contains not only the radio, but also the networking firmware needed to automatically form an IP-based mesh network. In addition, the LTP5901 has a built-in microprocessor which reads the LTC2484 ADC SPI port, and manages the power sequencing for the signal chain components. The LTC3330 is a low-power dual switch-mode power supply that derives power from the solar panel when enough light is available and reverts to using the battery when needed to maintain output voltage regulation. The LTC3330 also includes an LDO which is used to duty-cycle power to the temperature sensor.

*This article continues with a detailed description of the signal chain, including the analogue/digital conversion employed; the power demand, power provision and power management; and proceeds to the wireless networking part of the design. The author concludes by returning to the key issue of power, to look at the overall power usage of the circuit.*

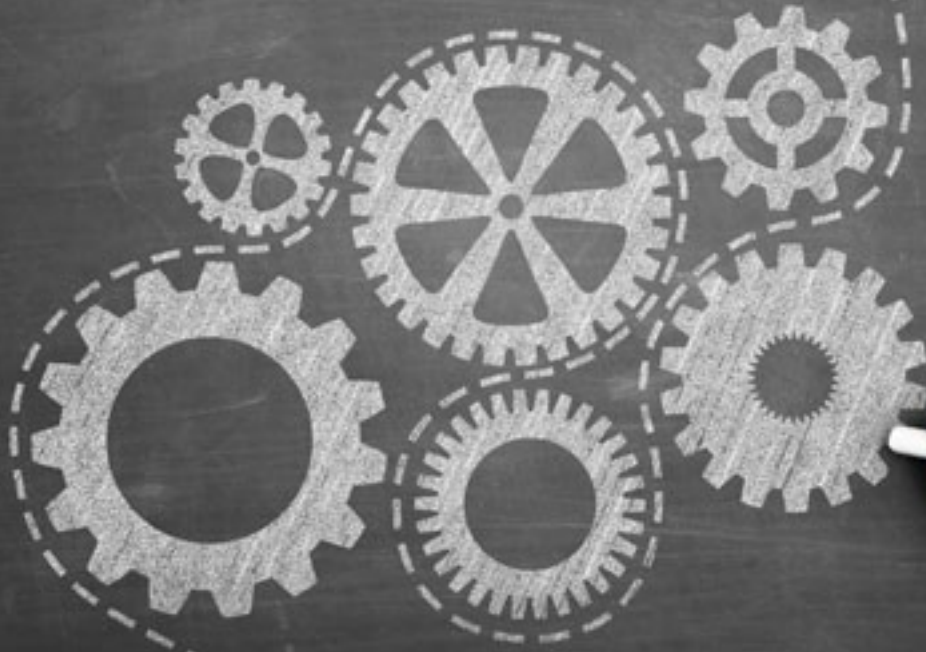


Download PDF  
of Article



Find wireless temperature  
sensors on EETsearch

# designideas



- Three-op-amp state-variable filter perfects the notch
- Series-connected MOSFETs increase voltage & power handling

## Three-op-amp state-variable filter perfects the notch By Alain Temps



The usual schematic of a state-variable filter with two inverting integrators is well known. Curiously, the input signal is almost always connected to the minus input of U1. Figure 1 is an example with  $\omega_0 = 1\text{ kHz}$  and  $Q = 5$ .

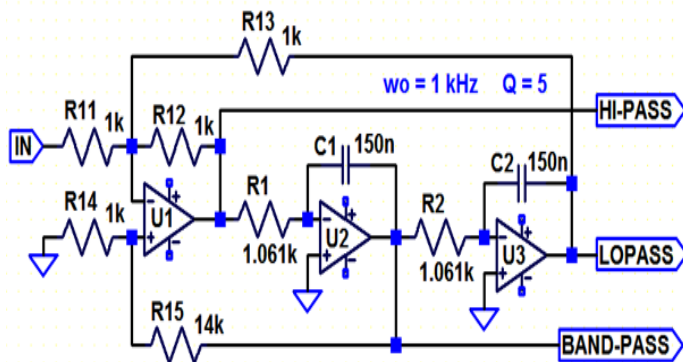


**Figure 1.** Typical state-variable filter

The circuit is known for its versatility, and ability to simultaneously provide low-pass, band-pass, and high-pass outputs. Gain, centre frequency, and  $Q$  may be adjusted separately. A notch filter is usually obtained by adding a fourth op-amp, either to sum the LP & HP outputs (which are out of phase), or to difference the input and BP outputs (which are in-phase). The notch depth then depends on

the matching of the resistances used for adding or subtracting the signals.

In this Design Idea, the input signal is instead connected to the positive input of U1; the filter naturally generates two notch outputs, without

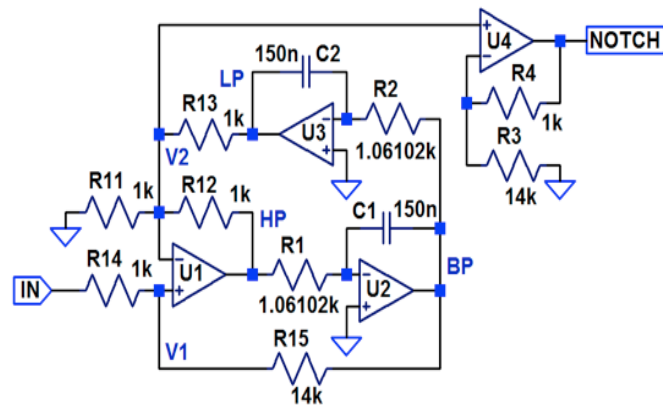


**Figure 2.** New state-variable design with two notch outputs

the need to combine any ports. These notch outputs are taken from the two inputs of U1, labelled V1 & V2. They are: the sum of the input and BP output for V1, and the sum of the HP & LP outputs for V2.

The complete equation is:

$$V_1/V_e = R_{15}/(R_{14}+R_{15}) [ 1 - \omega^2 R_1 C_1 R_2 C_2 R_{13}/R_{12} ] / [ 1 + j\omega R_2 C_2 R_{14}/(R_{14}+R_{15}) R_{13}/R_{123} - \omega^2 R_1 C_1 R_2 C_2 R_{13}/R_{12} ]$$

where  $R_{123} = R_{11} \parallel R_{12} \parallel R_{13}$

The numerator always has an exact zero at  $\omega_0 = 1/\sqrt{(R_1 C_1 R_2 C_2 R_{13}/R_{12})}$ .

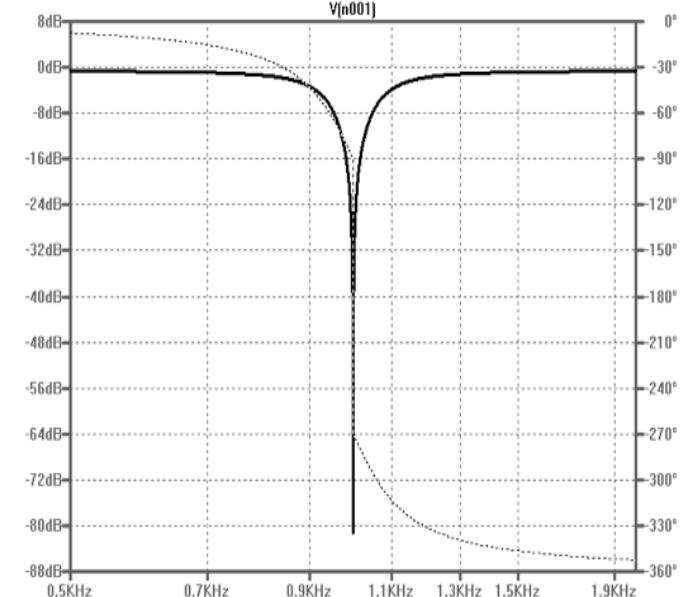


**Figure 3.** Notch frequency/phase response



Low frequency gain is always equal to high frequency gain, which means that rejection is naturally infinite at the centre frequency and does not depend on component tolerances. Amongst all notch filters, only the [Bainter](#) filter (and [here](#)) also possesses this property, but its parameters cannot easily be tuned separately.

Further equations:

$$Q_D = (1 + R_{15}/R_{14}) \sqrt{(R_1 C_1 / R_2 C_2)} / [ \sqrt{(R_{12} R_{13}) / R_{11}} + \sqrt{(R_{12} / R_{13})} + \sqrt{(R_{13} / R_{12})} ]$$

$Q_D$  is maximum, and the equations greatly simplify, if we choose  $R_{12} = R_{13}$ . Then:

$$V_2 / V_{in} = R_{15} / (R_{14} + R_{15}) [ 1 - \omega^2 R_1 C_1 R_2 C_2 ] / [ 1 + j\omega R_2 C_2 (2 + R_{12} / R_{11}) / (1 + R_{15} / R_{14}) - \omega^2 R_1 C_1 R_2 C_2 ]$$

LF & HF gain:  $A_0 = R_{15} / (R_{14} + R_{15})$

Notch frequency:  $\omega_0 = 1 / \sqrt{(R_1 C_1 R_2 C_2)}$  - may be tuned with  $R_1$  &  $R_2$

Q:  $Q_D = (1 + R_{15} / R_{14}) / (2 + R_{12} / R_{11}) \sqrt{(R_1 C_1 / R_2 C_2)}$  - may be tuned with  $R_{11}$

Practically, simulation shows that notch rejection is better on  $V_2$  than on  $V_1$ . It may exceed 80 dB with high speed op-amps at U2 & U3, and is limited by the op-amp specs.

Input impedance is not constant with frequency. However, neither rejection depth nor gain depend on source resistance, which appears in series with  $R_{14}$  and slightly decreases gain and  $Q_D$  (it is the same for Figure 1).

An optional buffer U4 with gain equal to  $(1 + R_{14} / R_{15})$  may isolate the filter from any external disturbance, and maintain gain at +1. The overall gain may of course be adjusted with  $R_3$  or  $R_4$ .

The output noise is extremely low across the whole spectrum; even lower at  $\omega_0$ .

For example, for U1, U2, & U3 with  $e_n = 5 \text{ nV}/\sqrt{\text{Hz}}$ , total noise at  $V_2 = 4.5 \text{ nV}/\sqrt{\text{Hz}}$  @  $\omega_0$  and  $6.4 \text{ nV}/\sqrt{\text{Hz}}$  in the rest of the spectrum.

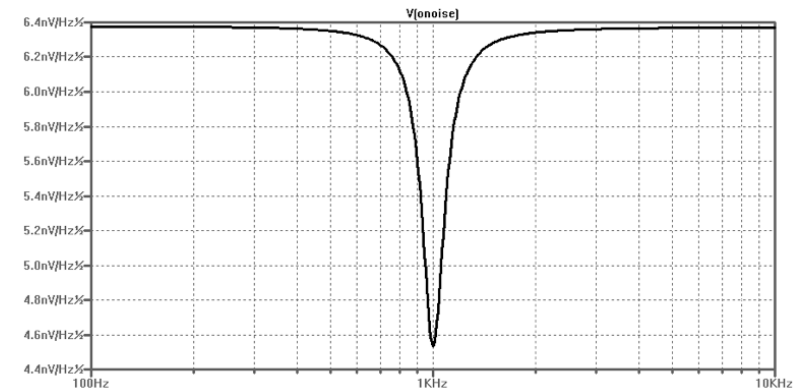


Figure 4. Noise vs. frequency

Be wary of possible saturation of U1 to U3 at centre frequency  $\omega_0$  because their gains are high if Q is high, as with any state variable filter.

The gains of U1-U3 at  $\omega_0$  are:

U1:  $- R_{15} / R_{14} \sqrt{(R_1 C_1 / R_2 C_2)}$

U2:  $R_{15} / R_{14}$

U3:  $(2 + R_{12} / R_{11}) / 2(1 + R_{14} / R_{15})$

Saturation characteristics may be improved by increasing the ratio  $C_1 / C_2$ , and/or decreasing  $R_{15} / R_{14}$ , at the expense of higher noise.

A [simulation](#) file can be downloaded. (Saved as a text file; delete any

### Series-connected MOSFETs increase voltage & power handling By Ilija Uzelac & Ron Reiserer



This Design Idea presents a simple, proven, reliable, and robust method for charging large capacitor banks, using a series connection of power MOSFETs to raise the breakdown voltage over that of an individual MOSFET.

When a power supply drives a large capacitive load the inrush current, if not limited, can reach tens or hundreds of amps for a high voltage power supply. In general, maximal ratings of a power supply could be transiently exceeded by many times, but this is generally acceptable when the transient lasts a few AC-line cycles. This is typical for load capacitances up to a couple of hundred microfarads, but for load capacitances in thousands of microfarads, an inrush current limiter is a must.

Using MOSFETs as voltage controlled current elements is very suitable for capacitor-charging circuit design. Consider though: If a task specifies charging a capacitor bank with 1A from rectified AC mains of 240V, a design with a single P-MOSFET would require that at power-on, the MOSFET pass 1A when its drain-to-source voltage  $|V_{DS}|$  is about 330V, which exceeds the safe operating area of most parts. For example, the IXTQ10P50P, at the maximum junction tem-

perature of 150°C, can handle 200 mA when  $|V_{DS}| = 250V$ , but over 2A when  $|V_{DS}| < 100V$ . This limitation can be overcome by connecting multiple P-MOSFETs in series.

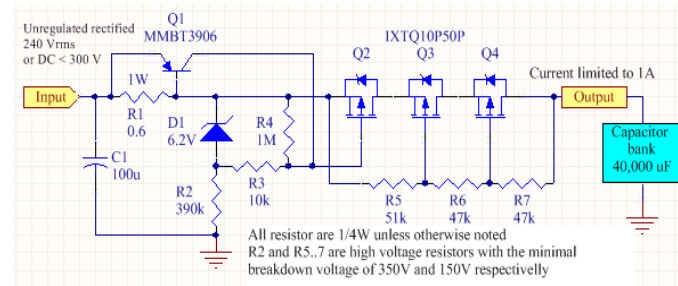


Figure 1.

Figure 1 shows a design with three P-MOSFETs connected in series. Neglecting the voltage drop across R1, the input voltage is approximately the same as the potential at Q2's source. Then, the gate potential of Q2 equals the input voltage minus 6.2V across Zener D1, and plus voltage drop across resistor R3. Resistors R5, R6, and R7 as voltage dividers ensure that the  $|V_{DS}|$  of each P-MOSFET is approximately equal – about 1/3 of the voltage difference between the input and output. R5 is purposely chosen to have a slightly higher resistance than R6 and R7 as the gate potential of Q2 is about 5V less than the input voltage. This correction equalises  $|V_{DS}|$  voltages even

more than if resistors R5, R6, and R7 were equal. R4 ensures that at power-on/off, Q2 is turned off.

At power-on, D1 provides 6.2V between the source and gate of Q2,  $|V_{GS2}|$ ; therefore Q2 is conductive. Q3 and Q4 are conductive as well, as the current through R5-R7 charges their gate-to-source capacitances. The capacitor bank charging current is sensed with R1 and regulated with the negative feedback control consisting of R1, Q1, R3, and Q2. When the voltage between the emitter and base of Q1 reaches  $V_{BE(on)}$  – that is, when the charging current is about 1A – Q1 starts to conduct. As  $|V_{GS2}| = 6.2 - R3 \times I_{C(Q1)}$ , any increase in  $I_{C(Q1)}$  decreases  $|V_{GS2}|$ . This decreases the output current, which in turn decreases the voltage across R1, completing the negative feedback loop.

Figure 2 shows voltage across the 40,000 μF capacitor bank as a function of time as the

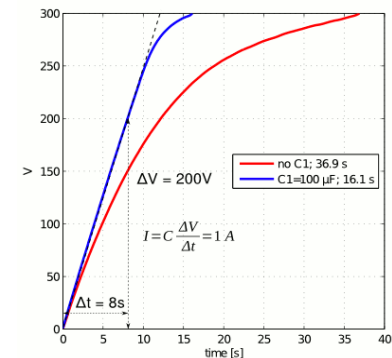


Figure 2.

capacitor bank is charged from 0V to 300V – for two different cases – with and without C1. Without C1, the capacitor bank is only partially charged during each rectified half-cycle – that is, when the input voltage is higher than the output voltage plus the voltage drop across all three MOSFETs of about 15V. Hence, the slope of the curve is not constant.

Adding C1 lets the charging circuit work with a more constant input voltage.

### Calculations for C1

C1 discharges at the rate of  $dV/dt = I/C = 10V/\text{msec}$ . This is almost an order of magnitude slower than the sinusoidal change of the input voltage from 330V to 0V that lasts 4.17 msec for 120 Hz half-cycles. Therefore, from the moment the input voltage reaches its maximum, the capacitor bank is charged only from the C1 capacitor until the input voltage exceeds the C1 voltage on the next rising slope of the 120 Hz period. As C1 is discharged with the constant current of 1A, the discharge time interval  $t_d$  is expressed as:

$$t_d = \frac{C}{I}(V_{max} - V_{C1}) \quad (1)$$

For this time interval, the input voltage changes from 330V to 0V and up to VC1:

Solving these two equations for VC1 shows that C1 discharges down to about 265V. As the voltage drop across three MOSFETs is about 15V, it follows that above 250V, the voltage across the capacitor bank doesn't increase linearly. This explains the variation from the linear dashed line in Figure 2.

This circuit is part of a complex device: our custom-built defibrillator for research studies [Ref. 1]. It has proven to work reliably for hundreds of cycles and hundreds of hours with numerous rapid discharges of the capacitor bank over the last two years. The circuit is tested up to an input voltage of 280 VRMS and works reliably with a heatsink temperature of up to 70°C. This Design Idea is not limited to the input voltage and current specified herein. The maximum input voltage and charging current can be raised with the addition of more P-MOSFETs in series. The downside is the voltage drop across each P-MOSFET of about 5V. Larger C1 capacitances than 100  $\mu\text{F}$  would linearise the charging curve at even higher voltages, or, of course, a DC input could be used.

### Addendum

The authors added this expansion on how (why) Q3 and Q4 are turned on; consider the initial case at power-on when the capacitor bank is discharged, that is when the output is at 0V. For the input voltage of 300V the gates of

Q3 and Q4 will be approximately at potentials of 200V and 100V. Q2 is initially conductive as it is biased with the Zener diode. If we assume that there is no current flowing through Q2, that is if Q3 and Q4 are off, then potential at the drain of Q2 (source of Q3) will be ~300V and voltage between the source and gate of Q3 will be ~100V; therefore Q3 must turn on, and Q4 subsequently.

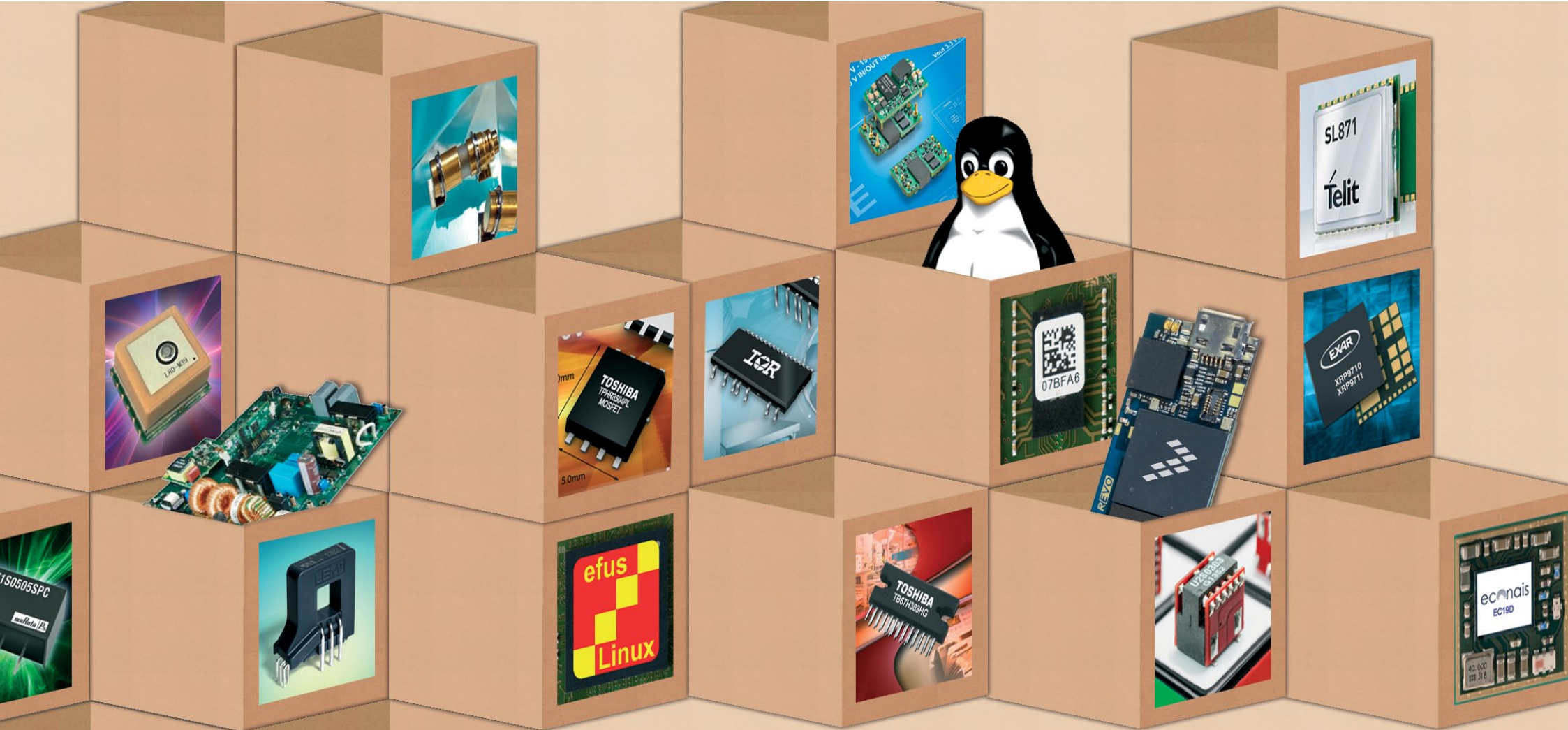
### Reference:

1. Uzelac I, Holcomb M, Reiserer RS, Fenton FH, Wikswo JP, [High-Power Current Source with Real-Time Arbitrary Waveform for In Vivo and In Vitro Studies of Defibrillation](#), Computing in Cardiology, 40:667-670, 2013

### About the Authors;

Ilija Uzelac is a Post-Doc at Georgia Institute of Technology, designing research instrumentation: microcontrollers, control systems, power electronic, sensors, measurements. Teaching: Industrial Control Systems, Electronics circuits. He holds BSEE/MSEE, and BSc/MSc and PhD degrees in Physics.





productroundup

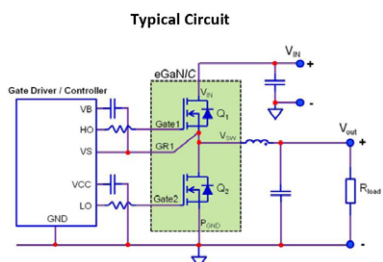


# productroundup

## GaN half-bridge betters 87%, 28V to 1V DC/DC at 14A

The EPC2101 GaN power monolithic half bridge, used in a complete point-of-load (PoL) buck converter, yields system efficiency that approaches 87% at 14A, and over 82% at 30A, when switching at 500 kHz and converting from 28V to 1V while reducing the board area occupied by transistors by 50% when compared to a discrete solution. EPC2101

is a 60V enhancement-mode monolithic GaN transistor half bridge. By integrating two eGaN power FETs into a single device, interconnect inductances and the interstitial space needed on the PCB are eliminated, resulting in a 50% reduction in board area occupied by the transistors.



Complete article, here



## Low-power FRAM for energy harvesting apps

Fujitsu Semiconductor's MB85RDP16LX is an ultra-low-power FRAM device with an integrated binary counter function. It incorporates multiple optimisations to reduce energy consumption to less than 10% of that required by standard FRAM solutions. With the MB85RDP16LX, Fujitsu is targeting industrial automation applications involving energy harvesting for rotary encoders, motor control and sensors. The ultra-low-power device can enable self-powering solutions such as the Wiegand wire-based platform being offered by iC-Haus. MB85RDP16LX replaces separate read/write operations with a single command from the MCU, resulting in energy savings of up to 94%.



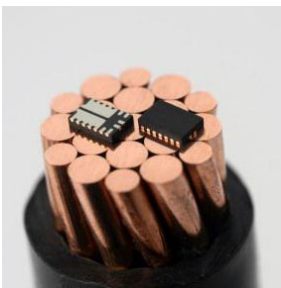
Complete article, here



## 10A power switch with accurate current sense

Silego Technology's 2.0 x 3.0 mm CurrentPAK SLG6M6001V enables high accuracy current measurement in a configurable and programmable 10A, 3.8 mΩ  $R_{DS(ON)}$  load switch. CurrentPAK is a family of configurable mixed-signal ICs, or CMICs. A high performance load switch that has efficient, high accuracy current measurement, CurrentPAK is

claimed as the first load switch to have advanced programmable features. Using non-volatile memory (NVM), designers can control several aspects of the device including enable logic, slew rate, current limiting, over-temperature protection, and integrated discharge rate. CurrentPAK SLG-6M6001V comes in a 2.0 x 3.0 mm, fully encapsulated, plastic package.



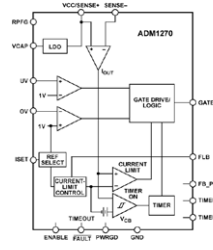
Complete article, here



## High-voltage inrush/overcurrent input protection

Analog Devices has posted details of the ADM1270, a current-limiting controller that provides inrush current limiting and overcurrent protection for modular or battery-powered systems. The ADM1270 is designed to control the inrush current, when powering-on a system, via an external P-channel field effect transistor (FET); it manages the currents that charge

bypass capacitors when circuit boards are inserted into a live backplane. These transient currents can cause permanent damage to connector pins, as well as dips on the backplane supply. To protect a system from a reverse polarity input supply, there is a provision made to control an additional external P-channel FET; use it in industrial modules, and in battery powered/portable instrumentation.



Complete article, here





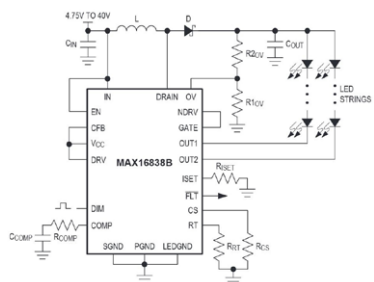


# productroundup

## 2-channel, high-brightness automotive LED driver

For use in automotive display backlights, automotive lighting applications and LCD backlights, Maxim has posted detail of the MAX16838B which it says is the only-available 2-string HB LED driver providing 10000:1 dimming ratio: the part has high-voltage boost and a SEPIC controller. The device is a dual-channel LED driver that inte-

grates both the DC-DC switching boost regulator and two 150-mA current sinks. A current-mode switching DC-DC controller provides the necessary voltage to both strings of HB LEDs. The MAX16838B accepts a 4.75V to 40V input voltage range and directly withstands automotive load-dump events.



Complete article, here



## NFC/FRAM/MCU transponder for industrial, medical, and wearable designs

Positioned as the first flexible high frequency 13.56 MHz sensor transponder family, TI's highly integrated ultra-low-power RF430FRL15xH system-on-chip (SoC) family combines an ISO 15693-compliant Near Field Communication (NFC) interface with a programmable microcontroller (MCU), non-volatile FRAM, an analogue-to-digital converter (ADC)

and SPI or I<sup>2</sup>C interface. The dual-interface RF430FRL15xH NFC sensor transponder is optimised for use in fully passive (battery-less) or semi-active modes in consumer wearables, industrial, medical and asset tracking applications.

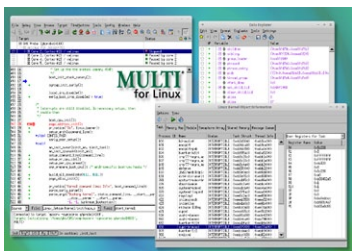


Complete article, here



## "Most powerful" embedded Linux C/C++ debugger

Green Hills Software has a new MULTI software development environment for embedded Linux developers; you can develop projects for the Internet of things, "cheaper and faster", the company asserts. Green Hills presents its MULTI as enabling developers to seamlessly control and debug all aspects of an embedded Linux system, including the Linux kernel, kernel threads, user mode threads and processes, and interrupt service routines (ISRs), all from a single tool. MULTI enables developers to quickly master development challenges including kernel panics, execution and data flows between user processes and the kernel, early hardware bring-up, device drivers, and performance analysis



Complete article, here



## FTDI Chip's HMI modules focus on capacitive touch

FTDI Chip has added development modules to accompany its Embedded Video Engine (EVE) modules, that employ an object-oriented approach to creating human machine interfaces (HMIs). The additional EVE platforms are targeted at the creation of intelligent display systems using capacitive touch and are based on the FT801 EVE chip released in 2014. Both of the new modules' touchscreens are able support from 1 to 5 independent touch points. The VM801B is a 106.7 x 68.6 mm development module with a choice of a 5 in. or 4.3 in. display, plus an integrated

projected capacitive touchscreen and a fitted, plastic bezel. The VM801P adds a built-in AT-MEGA328P Flash-based microcontroller.



Complete article, here

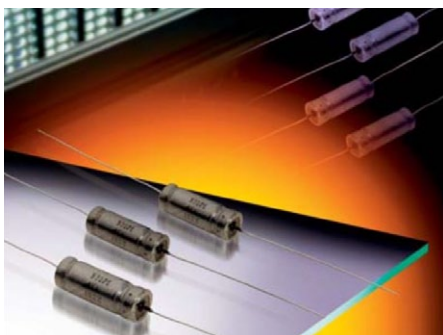






## 50 mF wet-tantalum capacitors challenge supercaps

**A**VX has developed a series of high CV wet tantalum capacitors that approach the ultra high volumetric capacitance densities of aqueous supercapacitors, as well as overcoming their temperature and soldering limitations. Developed using a design process based on high CV tantalum powders, the TWD DCUltraMax Series High CV Wet Tantalum Capacitors achieve extremely high DC capacitance values: unlike aqueous supercapacitors they are rated for continuous high temperature operation to at least +85°C and are compatible with both wave and reflow soldering to a PCB.

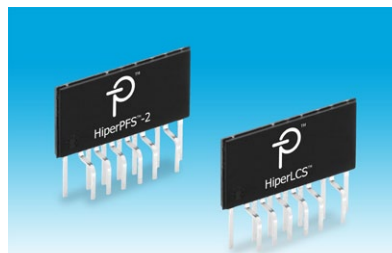


Complete article, here



## Reference design for high-power LED-lighting

**I**mproving efficiency, size and reliability of LED streetlights and high-bay lighting, the RDR-382 reference design describes a constant current, 43V (nominal), 150W reference power supply for 90-265 VAC solid-state lighting, using Power Integrations' HiperPFS-2 PFC controller ICs and HiperLCS integrated LLC power stage ICs. Traditional dual-stage drivers with separate PFC and LLC stages produce a constant-voltage (CV) output requiring multiple DC-DC converters to convert the output to constant current (CC). In contrast, RDR-382 uses a novel feedback and control scheme which enables the LLC to provide constant current directly at the output.



Complete article, here



## ARM mbed Bluetooth & WiFi boards from CSR

**C**SR offers two connectivity products for the ARM mbed operating system that will enable developers to produce complete Internet of Things (IoT) solutions. CSR will offer two mbed expansion boards, also known as shields; one combines Wi-Fi and Bluetooth based on the CSR6030 and CSR8311 ICs. The other offers Bluetooth Smart connectivity based on a CSR1010 chip. These shields, which will be released in early 2015, are designed to work with the ARM mbed OS that will also be available to developers in early 2015. The two systems will provide the fundamental connectivity required for all IoT devices.



Complete article, here



## Multi-function MEMS sensor integrates gas sensor

**T**his environmental sensor from Bosch Sensortec combines pressure, humidity, temperature and indoor air quality measurement parameters. You can use it to equip mobile devices and wearables with indoor air quality measurement, with its low power consumption and small package. BME680 integrates a gas sensor with full-specifications air pressure, humidity and ambient air temperature sensing functions in a single 3.0 x 3.0 mm footprint. The gas sensor within the BME680 can detect a broad range of gases in order to measure indoor air quality for personal well-being, including Volatile Organic Compounds (VOC) from paints.



Complete article, here





# productroundup

## ST updates Bluetooth network processor to BT4.1

**S**TMicroelectronics has released the latest version of its BlueNRG Bluetooth SMART network processor, which supports the latest Bluetooth version 4.1 enhancements and introduces 1.7V operation for longer-lasting battery-powered applications. The BlueNRG-MS network processor integrates a complete Bluetooth PHY and 2.4GHz radio, ARM Cortex-M0 microcontroller running the Bluetooth 4.1 protocol stack, and dedicated AES-128 security coprocessor. The API, power management, and Flash are already integrated, allowing direct connection to the application host controller using a simple SPI bus using clear software partitioning between network processor and host microcontroller. ST's BlueNRG-MS network processor can power devices such as a hub capable of collecting sensor data and subsequently acting as a peripheral to transfer the data to a smart phone. It can also allow very large sensor networks with unlimited communication range, controlled by a single smartphone.

[Complete article, here](#)

## Raspberry Pi/Arduino-based project case

**H**ammond Electronics' 1593HAMEGG enclosures are board-specific designs that provide a ready-made housing for the Arduino and Raspberry Pi bareboard computers. Available in translucent blue, translucent purple or translucent black, they have been designed to provide an alternative to traditional base and lid designs where the bareboard is mounted inside an enclosure. The new cases are configured for the Raspberry Pi A, A+, B and B+ and the Arduino Uno, Due, Ethernet, Leonardo, Mega ADK, Mega 2560 and Yún. Board-specific versions for designs from other manufacturers active in this sector are in development.



[Complete article, here](#)

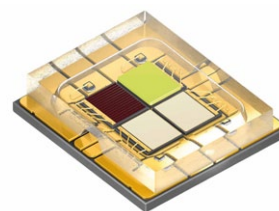
## 10-Watt class, wireless power chipset

**T**oshiba Electronics Europe has a wireless power receiver IC, TC7765WBG, and a transmitter IC, TB6865AFG Enhanced Version, that together comprise a 10-W-class wireless power solution for smartphones, tablets and mobile accessories using the Qi Standard Low Power Specifications version 1.1, defined by the Wireless Power Consortium (WPC). The receiver IC, TC7765WBG, increases power by boosting the output voltage from 5V/1A to 7-12V/1A. The transmitter IC, TB6865AFG Enhanced Version, realises a 10-W-class wireless power solution based on a revised peripheral circuit configuration and new software. The TC7765WBG's built-in protocol authentication logic circuit for power supply control eliminates the need for set makers to develop software. The TB6865AFG Enhanced Version also supports the software necessary for the higher power supply operation.

[Complete article, here](#)

## 4-colour LED module: high lumen output

**D**istributor Rutronik has the Osram Ostar Stage LED from Osram Opto Semiconductors. Compared with previous members of the product family, it offers more than twice the lumen output, whereas the component surface is only 30% larger. The Osram Ostar Stage is equipped with four high-current chips based on the latest thin-film and UX:3 chip technologies. With an area of 2mm<sup>2</sup> each, the chips are twice as large as the previous ones, but at 5.7 x 6.4 x 1.3 mm, the package size is only slightly larger. Thin-film chips in red (625 nm) and UX:3 chips in green (530 nm), blue ("deep blue": 453 nm) and white are used. Up to 4.5A can be applied to each chip, which allows more light to be produced from a small surface.



[Complete article, here](#)

# REVIEW

## TEKTRONIX RSA306 SPECTRUM ANALYSER

BY KENNETH WYATT, EDN

The spectrum analyser has always been a vital tool for the EMC engineer. Until the last few years, these instruments have been rather large and heavy desktop instruments, weighing up to 30 kg, or more. With the breakthroughs in components used for wireless technology, the size and weight of these instruments has decreased dramatically.

A few other manufacturers have pioneered the concept of PC-controlled spectrum analysers and Tektronix has recently entered the fray with its RSA306, which has dramatically raised the bar in terms of performance and measurement capability. The RSA306 is a well-built rubber-covered unit that is about the size that will slip into the jacket pocket of your suit (30 x 190 x 127 mm). It would also fit easily into a briefcase along with a 15-inch PC laptop. It is designed to meet MIL-STD-28800 Class 2 environmental, shock and vibration for use in harsh environments. The RSA306 is powered solely through the USB 3.0 port. The frequency range is 9 kHz to 6.2 GHz and can measure from +20 to -160 dBm (at minimum resolution bandwidth of 100 Hz). The unit can capture fast transient pulses with its 40 MHz real-time IF bandwidth.

There are also external 10 MHz reference and trigger/sync SMA inputs, so you can sync to line frequencies, for example. The measurement input is an N connector with protective

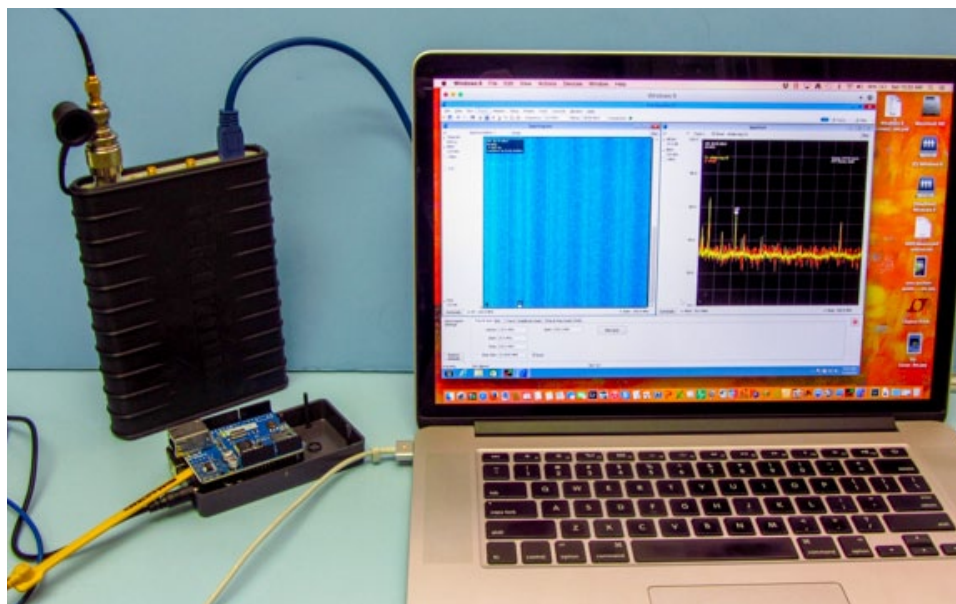


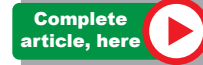
**Figure 2.** The RSA306 connected to a Mac laptop running Windows 8. The harmonics from an Arduino controller are being measured. The regular spectrum and waterfall are displayed.

rubber cap. With all this, Tektronix has been able to keep the cost down to just €2,810 for the basic unit. Included in this price are a safety/installation manual, USB 3.0 cable and USB flash drive containing the documentation files,

user manual, drivers and SignalVu-PC software.

One reason for the low cost is that much of the functionality lies in the SignalVu-PC RF analysis software. The software includes 17 standard spectrum and signal analysis measurements, with several optional application-specific options available (€757, each). These options include mapping, modulation analysis, standards support (such as APCO P25 and WLAN), pulse measurements and frequency settling. The real time (DPX mode) can detect transient or intermittent signals as short as 100 µsec, which would aid in interference hunting. The software can also capture streaming and audio demodulation for long-term surveillance monitoring. Because the personality of the instrument lies within the software, upgrades and adding optional measurement capabilities are easy.

*In the complete article (click right) the author looks at PC host requirements, reviews the capabilities of the instrument, then gets down to making some real-world measurements.*





# EDN

## europe

**EDN-EUROPE** is published 11 times in 2015 by  
**European Business Press SA,**

7 Avenue Reine Astrid, 1310 La Hulpe, Belgium

Tel: +32-2-740 00 50 Fax: +32-2-740 00 59

email: [info@eetimes.be](mailto:info@eetimes.be).

VAT Registration: BE 461.357.437.

RPM: Nivelles.

It is free to qualified engineers and managers  
involved in engineering decisions – see:

<http://www.edn-europe.com/subscribe>

Copyright 2014 by European Business Press SA.

All rights reserved. P 304128

### CONTACTS

#### PUBLISHER

André Rousselot

+32 27400053

[andre.rousselot@eetimes.be](mailto:andre.rousselot@eetimes.be)

#### CIRCULATION & FINANCE

Luc Desimpel

[luc.desimpel@eetimes.be](mailto:luc.desimpel@eetimes.be)

#### EDITOR-IN-CHIEF

Graham Prophet

+44 7733 457432

[edn-editor@eetimes.be](mailto:edn-editor@eetimes.be)

#### ADVERTISING PRODUCTION & REPRINTS

Lydia Gijsegom

[lydia.gijsegom@eetimes.be](mailto:lydia.gijsegom@eetimes.be)

Patrick Mannion

Brand Director EDN Worldwide

#### ART MANAGER

Jean-Paul Speliers

#### ACCOUNTING

Ricardo Pinto Ferreira



european  
business press

### SALES CONTACTS

#### Europe

Daniel Cardon

France, Spain, Portugal

+33 688 27 06 35

[cardon.d@gmail.com](mailto:cardon.d@gmail.com)

Nadia Liefsoens  
Belgium

+32-11-224 397

[n.liefsoens@fivemedia.be](mailto:n.liefsoens@fivemedia.be)

Nick Walker  
UK, Ireland, Israel,  
The Netherlands

+44 (0) 1442 864191

[nickwalker@btinternet.com](mailto:nickwalker@btinternet.com)

Victoria & Norbert Hufmann  
Germany, Austria,  
Eastern Europe

+49 911 93 97 64 42

[sales@hufmann.info](mailto:sales@hufmann.info)

Monika Ailinger  
Switzerland

+41-41-850 4424

[m.ailinger@marcomedia.ch](mailto:m.ailinger@marcomedia.ch)

Andrea Rancati  
Italy

+39-02-284 6716

[info@silvera.it](mailto:info@silvera.it)

Colm Barry & Jeff Draycott  
Scandinavia

**+46-40-41 41 78**

[jeff.draycott@womp-int.com](mailto:jeff.draycott@womp-int.com)

[colm.barry@telia.com](mailto:colm.barry@telia.com)

#### USA & Canada

Todd A. Bria  
West

+1 831 477 2075

[tbria@globalmediasales.com](mailto:tbria@globalmediasales.com)

Jim Lees  
PA, NJ & NY

+1-610-626 0540

[jim@leesmedia.com](mailto:jim@leesmedia.com)

Steve Priessman  
East, Midwest,  
South Central  
& Canada

+1-630-420 8744

[steve@stevenpriessman.com](mailto:steve@stevenpriessman.com)

Lesley Harmoning  
East, Midwest,  
South Central  
& Canada

+1-218.686.6438

[lesleyharmoning@gmail.com](mailto:lesleyharmoning@gmail.com)

#### Asia

Keita Sato  
Japan

+81-3-6824-9386

[MIshida@mx.itmedia.co.jp](mailto:MIshida@mx.itmedia.co.jp)

Grace Wu  
Asian Sources Publications  
Asia

(886-2) 2712-6877

[wug@globalsources.com](mailto:wug@globalsources.com)

John Ng  
Asian Sources Publications  
Asia

(86-755) 8828 – 2656

[jng@globalsources.com](mailto:jng@globalsources.com)